SLOPE STABILITY ANALYSIS OF THE BOZSHAKOL OPEN PIT MINE USING THE FINITE ELEMENT METHOD

by

TOREKELDI MARATOV

THESIS SUPERVISOR

Professor ALI MORTAZAVI

Thesis submitted to the School of Mining and Geosciences of Nazarbayev University in Partial Fulfillment of the Requirements for the Degree of

Bachelor of Science in Mining Engineering

Nazarbayev University

07.04.2023

ORIGINALITY STATEMENT

I, Torekeldi Maratov, hereby declare that this submission is my own work and that, to the best of my knowledge, it contains no materials previously published or written by another person or substantial proportions of material that have been accepted for the award of any other degree or diploma at Nazarbayev University or any other educational institution, except where due acknowledgement is made in the thesis.

Any contribution made to the research by others, with whom I have worked at NU or elsewhere, is explicitly acknowledged in the thesis.

I also declare that the intellectual content of this thesis is the product of my own work, except to the extent that assistance from others in the project's design and conception or in style, presentation, and linguistic expression is acknowledged.

Signed on 07.04.2023

_____

ABSTRACT

Slope stability analysis is a key part of every geotechnical problem of various extents. Ensuring an appropriate analysis enables sustained production and a safe environment at the mine site. In regard with the thesis research, a two-dimensional finite element method is selected for the analysis of the Bozshakol open-pit mine. In the process, all production stages are analyzed using numerical calculations. Particularly, the south wall of the pit is most concerning, as it appears to be the critical zone susceptible to possible instabilities based on the compiled data. Initially, the results of mining activities include uplift from the pit bottom and downslides of rock from the lateral walls of the pit section (e.g., excavation, blasting, benching). The numbers and visuals show that this pattern is prevalent throughout the production phases. Most importantly, higher displacements and deformations are observed along the south wall of the pit than along the north wall. With the critical SRF, as in production stage 2, the south wall moved as much as 0.035 m, while the north wall moved as little as 0.008 m. The rock movement was found to be 3.26 m as SRF was increased to a maximum of 2.6. This pattern necessitates keeping SRF and FoS values around or below the crucial value (2.15-2.21). In addition, as the production stages advance, we expect the maximum rock movement to increase from 0.035 to 0.142 meters from stage 2 to stage 6 if critical FoS are kept. Since total displacement fields grow proportionally as mining progresses, it is crucial to deal with potential problems as soon as they arise. Ultimately, the location of gabbro is indicative of the most active zone of displacement. As a result, this points to flaws in the rock influencing this result, which are the low intact rock and rock mass properties. Further three-dimensional research and improved sensitivity analysis are recommended for the advancement of the project.

ACKNOWLEDGMENT

I would like to express my gratitude to KAZ Minerals and The Bozshakol Copper Mine for providing me with the opportunity to access and make use of the geological and geotechnical data pertaining to their respective mines for the purpose of this research endeavor. I would like to extend my sincerest gratitude to Bayuprima Adiyansyah, the geotechnical supervisor at the mine, as well as Jose Gonzalez Borja, the geotechnical manager, for the support they provided in compiling these data.

My supervisor, Professor Ali Mortazavi, is someone I owe an enormous debt of gratitude to, and it is something I will always appreciate. Because of his support and direction, I was ultimately successful in completing my BSc thesis within the allotted time frame.

I would like to express my gratitude to my family, who have provided me with unwavering support throughout the duration of this study project.

TABLE OF CONTENTS

LIST OF FIGURES

LIST OF TABLES

1. INTRODUCTION

1.1 Background

Throughout the history of geotechnical engineering, slope stability analysis has always been a pivotal point in the design of civil and mining constructions. Surface mining, including the open-pit method, requires an extensive and thorough geotechnical investigation before and during production to ensure the best safety conditions (Read & Stacey, 2009). In that regard, engineers must pay attention to the accurate evaluation of the overall slope angle, bench face angle, bench height, berm width, and final pit shape to prevent any accident that may result in the loss of lives or significant downtime. In practice, mining companies typically face five general types of failures, such as circular, planar, toppling, and complex (Read & Stacey, 2009; Martin & Stacey, 2017). Each of the modes, however, has a different failure mechanism and level of risk it imposes on the pit.

The slope stability analysis itself has been modified and refined multiple times by implementing new and more effective computational tools. In that regard, the foremost and simplest one is the empirical method. It is commonly described as an experience-based, low-cost, and time-efficient approach (Bar & Barton, 2017; Read & Stacey, 2009; Matthews et al, 2014; Han et al, 2001). Empirical models, as their name suggests, are established on the basis of visibly perceptible real-life measurements. These measurements are typically collected from a limited number of geotechnical slopes. Such a practice, therefore, leads to lowered flexibility and versatility of the approach. The empirical data collected from Canadian mines, for example, cannot be reliably projected or used on Kazakhstani ones, and vice versa. Nowadays, empirical models are widely used for simpler bench or preliminary slope design problems given their aforementioned advantages (Bar & Barton, 2017; Han et al, 2001). The drawbacks, however, make it significantly inferior to more advanced tools such as analytical, limit equilibrium, and numerical methods. Analytical and limit equilibrium methods are oftentimes deemed as interim solutions between simple empirical methods and complex numerical calculations. Accordingly, they are used for geotechnical problems of intermediate difficulties, such as hydrogeological issues and dewatering rates.

In that sense, the Bozshakol copper mine is a perfect place to evaluate the state of the slopes using numerical analysis. Yet, the company has been running conventional preliminary studies using a simplistic approach in the form of limit equilibrium and analytical tools prior to and during production. Although these traditional solutions might be sufficient for the copper mine's relatively shallow depth (-400 m), the large production scale and unconventionally intricate shape (i.e., not circular) of the mining induces the need for more rigid contemporary tools. In particular, the factors of safety and kinematic analyses conducted for the individual geotechnical sectors may not represent the entire state of the pit. For example, the guidelines on interpreting safety factors for surface mining vary from one author to another. However, the safety factor of 1.2 is oftentimes considered minimal and accordingly implies the need for support or a slight geotechnical design adjustment (Martin & Stacey, 2017; Read & Stacey, 2009). As low as this factor goes, the slope may be more susceptible to different types of failures, which might ensue a production halt and safety risks for the workers. Moreover, given the inability to provide more information on possible solid displacements, deformation contours, and mining-induced stress levels in-between the production phases, limit equilibrium methods seem narrow for the scale of work being conducted in Bozshakol.

Nowadays, this problem can be efficiently managed with the introduction of numerical methods as more companies switch to that kind of approach. In terms of offering analysis on different scales, the numerical analysis provides both a two-dimensional and three-dimensional look at stress levels. The more companies invest in three-dimensional numerical analysis, the better and more extensive results they are likely to obtain. This thesis, nevertheless, primarily focuses on two-dimensional analysis as it makes possible extensive research around the critical zones or walls of Bozshakol. A three-dimensional analysis is accordingly deemed possible and recommended after this study. Finite-element modeling, on the other hand, is one of the most popular tools used in numerical simulations. The dominance of FE has been recognized in many engineering disciplines, including geomechanics and geotechnical engineering (Griffiths & Lane, 2001; Rao, 2018).

1.2 Objectives of the Thesis

1.2.1 Main Objectives

- The thesis primarily aims at delivering the results from numerical analysis as opposed to conventional limit equilibrium and analytical tools. From this, the levels of safety of the pit walls should be identified.
- The secondary goal of the thesis is to reveal the deformation prone zones and mechanisms of possible failures.
- Thirdly, the alteration of the rock strength parameters to different extents should display the sensitivity of the model.

1.2.2 Specific Objectives

- Analyze the effects of changes in mechanical and strength parameters of different rocks (i.e., cohesion, friction angle, elasticity modulus, peak tensile strength) on wall behaviour.
- Evaluate the safety level of the Bozshakol open-pit wall with regard to the wall displacement and stress fields, and deformation contours at each individual stage of the pit expansion.
- Evaluate the changes in-between the stages and determine any observable trend in safety level given the time dimension.
- Estimate the sensitivity of the model to different levels of changes in elasticity modulus, cohesion, and friction angle.
- Determine any observable critical zones in the model while presenting the chosen two-dimensional section of the pit.

1.3 Hypotheses

The pre-modelling stage involved a series of assumptions regarding the simulation outcome. These assumptions concerned safety conditions, critical zones of the wall, and overall stress levels. Most importantly, however, was to ensure that the results could not be easily assumed

or predicted as it might stand as a major sign of data manipulation and prejudice towards the end product.

The original hypotheses look as follows:

- The south wall of the pit might be more critical and prone to failure modes as opposed to the north wall due to the low strength parameters of the gabbro.
- The overall solid displacement levels at critical SRF might be fairly high (e.g., 1-2 meters) due to the weak rocks included in the model.

1.4 Justification of the R&D

It is worth admitting that KAZ Minerals Bozshakol has conducted a series of preliminary and extensive studies on the geotechnical aspects of the production to ensure the best safety measurements on the site. That includes empirical, analytical, kinematic, and limit equilibrium calculations using advanced contemporary tools and software. The geotechnical department of KAZ Minerals Bozshakol, however, is interested in numerical tools, including finite-element modelling. The two-dimensional analysis is expected to provide substantial information on solid deformation and displacements throughout the production stages. In addition to being elaborate, such a method is relatively user-friendly and interactive. If major deformations/displacements are revealed, a convenient support system can be designed using this tool.

1.5 Scope of Work

The scope of work around the thesis comprises multiple interrelated steps. It includes both primary and secondary research on slope stability analysis, numerical calculations, finite elements, and the Bozshakol copper mine. In particular, the following actions are undertaken to perform the work:

- Conduct a thorough review of existent scientific articles, papers, and books on slope stability analysis and numerical methods to collect as extensive and as reliable information as possible.

- Collecting and sorting out the essential data on the Bozshakol mine. That is, laboratory data, geotechnical sectors map, intact rock parameters, pit geometry, groundwater conditions, and the production phases.
- Acquiring the necessary rock mass parameters through RocLab simulation
- Use of the collected data within the RocScience RS2 environment and wall scale numerical modelling of Bozshakol pit.
- Interpretation of the results on solid displacements (e.g., vertical, horizontal), deformation contours, and stress levels.
- Sensitivity analysis by changing the rock strength parameters to different extents.

2. LITERATURE REVIEW

2.1. A Brief Overview of Slope Stability

Slope stability is a vital geotechnical aspect of every open-pit mining project. Disregarding or insufficient analysis of slope stability may result in consequent instabilities and even slope failure. A slope stability analysis in turn assists in terms of planning a geotechnical safe mine project and controlling weak zones of the pit during the process. There are fundamental types of slope stability analysis such as empirical, analytical, limit equilibrium, and numerical methods. In every open-pit mining project, an appropriate pit slope design is a priority in terms of providing the best excavation arrangement favoring both economic and safety aspects of the production. Improper-designed pit slopes may have failures of various extents triggering both economic (e.g., loss of equipment) and safety conditions (e.g., loss of worker life and company reputation), which inevitably impose financial losses on the project (Read & Stacey, 2009). The review and guidelines of Read & Stacey (2009) on slope stability encompass both fundamental and up-to-date information in regard to important mining topics such as structural, rock mass, geological, geotechnical, and hydrogeological models. These are the significant subjects that embody the research & development of this thesis. Martin & Stacey (2018), on the other hand, provide a piece of vital knowledge on the open pit design methods for weak rocks. Taking into

account that the Bozshakol open pit may have weak rocks, including young sedimentary rocks, the use of these guidelines may be advantageous.

2.2. Empirical Methods

Empirical methods are experience-based models used for preliminary analysis of most geotechnical problems. It is indeed a fairly simple, low-cost, and fast approach. Various experiential rock slope engineering methods can be utilized in the initial rock slope design. During the earlier stages, slope heights and slope angles might be calculated from these empirical charts (see Fig. 1). The q-slope engineering method is one of them, and it allows engineers to adjust the pit wall angle depending on the rock conditions revealed throughout the course of development (Bar & Barton, 2017), as illustrated in Fig. 2. The q-slope method prevails over numerical and analytical methods in terms of quick and timely evaluations made in response to the excavation progress. It provides an early representation of stress levels and allows subsequent prevention of unnecessary bench failures. Q-slope as well as any empirical model is not proposed as being rigorous, as such. For more complex problems like monitoring wedge stability, instead, analytical and numerical methods are suggested. They are, in turn, costly, time-consuming, and complicated. Given the insufficient amount of data that can be used for either limit equilibrium or numerical methods, the employment of empirical models can be a convenient solution. It can be helpful for initial slope designs (Read & Stacey, 2009; Jing & Hudson, 2015; Bar & Barton, 2017). Moreover, Jing & Hudson (2015) highlight the fact that engineering, in a broader sense, always faces with a lack of required data for an accurate analysis. That is why, as the authors assume, empirical charts and models keep being essential in rock mechanics. In addition, this paper presents eight global approaches toward slope stability analysis based on four basic tools (i.e., empirical, LEM, analytical, numerical) and two mapping levels. In regard to the thesis, Method C seems the most convenient between these approaches, as it covers finite elements modelling.

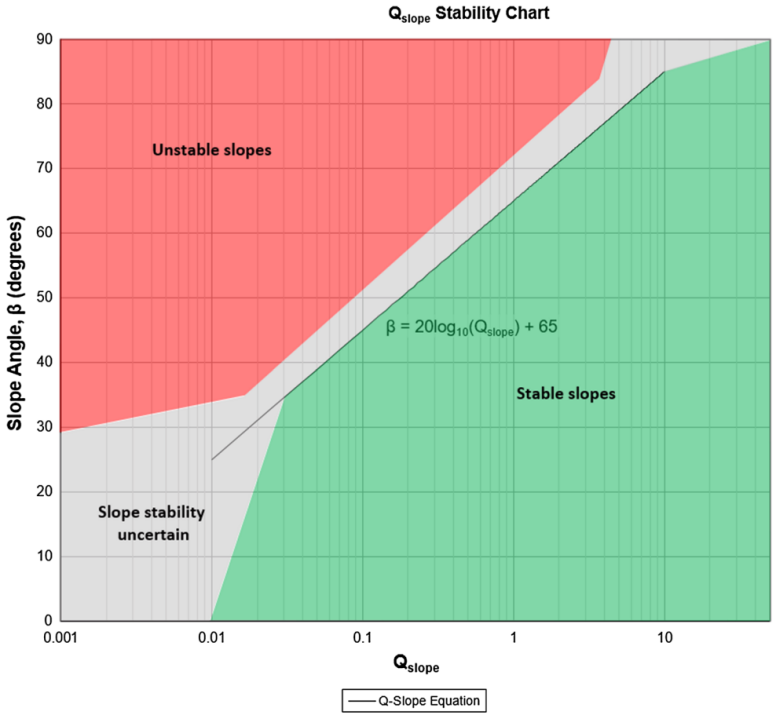

Figure 1. Q-slope stability chart (Bar & Barton, 2017)

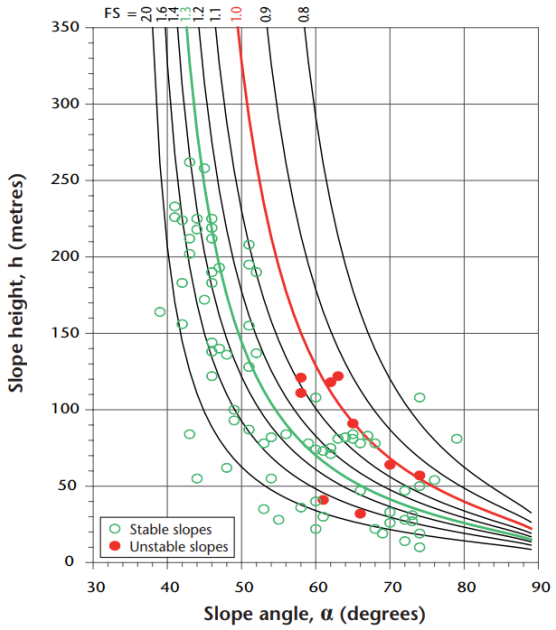

Figure 2. Rock slope versus slope height, distinguishing between failures and non-failures (Read & Stacey, 2009)

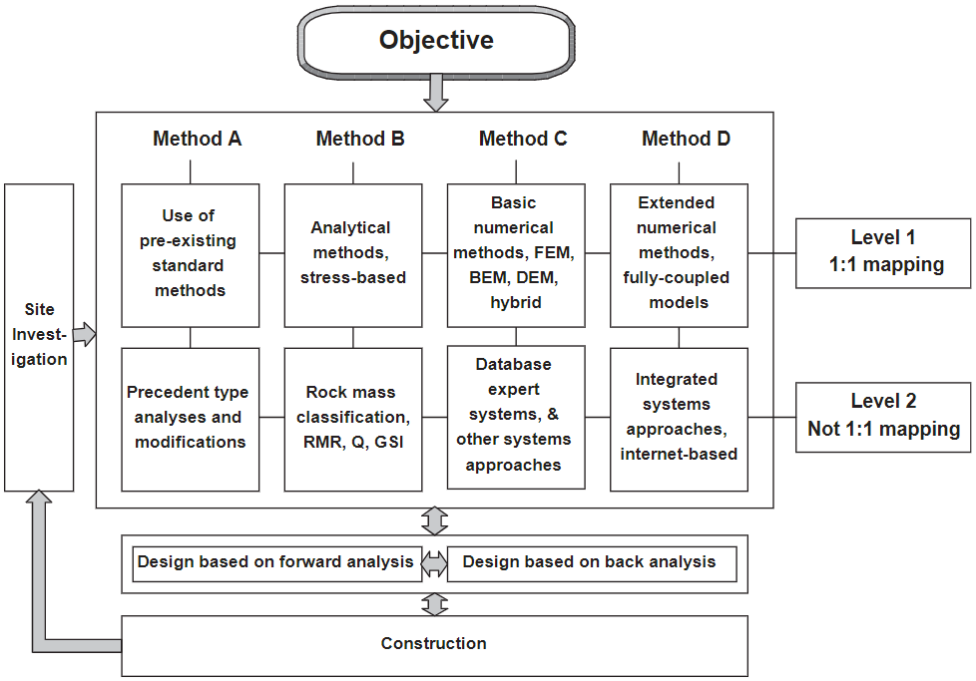

Figure 3. Eight approaches for rock mechanics modelling (Jing & Hudson, 2015)

As opposed to these advantages, the major limitation of the empirical approach is that it is contextual and cannot be effectively utilized under different circumstances. The empirical model developed in one country may not be valid for another. Also, the semi-quantitative nature of the models induces secondary analysis to achieve more reliable results. Read & Stacey (2009), for example, emphasize that Haines and Terbrugge graph falsely assumes the calculation of slope angles and slope heights only relying on the MRMR rating of the rock mass. It may, in fact, require thorough analyses afterward. Since the method provides solely a conceptual and precursory design of the pit slope, it might also need further analytical or advanced approaches (e.g., limit equilibrium, numerical modelling) for a sufficiently higher level of certainty of failure prevention within the scope of slope stability analysis.

2.3. Limit equilibrium Methods

Unlike other methods, limit equilibrium models heavily focus on the stability of sliding planes. The popular safety factor approach has become the common stability indicator in the industry.

The papers of Liu et al (2015), Read & Stacey (2009), and Matthews et al (2014) commonly highlight the easiness and simplicity of the approach. This is justified by the simplified assumptions used in the determination of the safety factor. The most common types of limit equilibrium models are the method of slices, Bishop simplified, and Morgenstern-Price methods (Liu et al, 2015; Chiwaye, 2009). The method of slices is the oldest and simplest limit equilibrium solution albeit ignoring possible interslice forces and does not represent the force equilibrium in regard to the sliding body. Bishop's simplified method also disregards interslice forces and includes a limited number of unknowns. In contrast to the method of slices, Bishop's simplified does not meet force equilibrium for one of the slices. Both of them, nonetheless, satisfy moment equilibrium. Between limit equilibrium and numerical solutions, several differences are observed. It is apparent that numerical modelling prevails over LEM in terms of higher accuracy and better performance for complex rock slope engineering problems. Matthews et al (2014), moreover, reveal the proximity between the results of Bishop and Fellenius methods. The assumption is backed by the early studies of Duncan (1996), who determined a mere 6% difference across these methods. Although limit equilibrium methods still dominate in the field, Matthews et al (2014) justifiably mention the importance and growing popularity of numerical calculations given the modern computational advantages. Most relevantly here, the authors emphasize the point, beyond which limit equilibrium is no longer an all-powerful tool. That is a complex geotechnical problem with a potential severe deformation that needs a highly realistic analysis of the situation. Numerous papers (Liu et al, 2015; Chiwaye & Stacey, 2010) already underline the benefits of the limit equilibrium approach for the bench design but often fails to clarify the relevance of the method for large mines with an intricate geometry. Furthermore, according to the study of Liu et al (2015), both of the examined FE (i.e., enhanced limit strength method and strength reduction method) resulted in closer safety factor values in comparison to the conventional limit equilibrium model. Although the safety factor may not look rigorous, it has been a stability indicator for most of the geotechnical problems in the industry. Minimum, maximum, and mean accepted factors of safety can be arranged depending on the project scale and the consequences of the failure that may occur. For example, every individual bench is expected to have a mean FS of 1.3, a permanent slope FS of 1.6, and high slopes upon which haulage ramps are situated should have

an average of 2.0 FS. Nevertheless, Wiles (2006) specifies that the term "safety factor" as defined above cannot be utilized to make meaningful comparisons between different scenarios. FS measured in the Bozshakol copper mine, for example, may not provide a unique and precise illustration of safety conditions. Thus, it cannot be compared to those measured in other open-pit mines. The outcome, as Wiles (2006) contributes, will still be affected by the local value of principal stress sigma 3, even though the amount of the safety factor may be modified to offer the same likelihood of failure depending on local site conditions. The application of probability approaches can eliminate this source of uncertainty in the modeling predictions.

2.4. Analytical Methods

Analytical or kinematic solutions have been widely used for detecting failure mechanisms of a rock slope. Mostly, kinematic methods utilize stereographic projection techniques to determine various types (e.g., planar, wedge, and toppling) of failure, according to Obregon & Mitri (2019). The thesis also addresses the two-stage process involved in the research of kinematic methods. It initially examines the structural features of the rock mass to reveal potential displacements across the mine slope. Given the results of the primary step, the relation between the rock strength and imposed stress is examined to calculate the safety factor. Safety factor (or Factor of Safety), as mentioned earlier, is an important tool for ordinary geotechnical problems. Notwithstanding the advantage of numerical methods over kinematic ones, the thesis does not identify the weaknesses of the chosen approach. It is, instead, labeled as a prominent method for mine slope failure analysis. Analytical methods are classified as deterministic and probabilistic depending on the assumptions. The deterministic kinematic approach refers to average discontinuity sets that lie beyond the critical zones, whereas probabilistic analysis is more useful for occasions when the orientations of the discontinuities are instead located within this instability zone.

2.5. Numerical Modelling

Numerical modeling has been used widely for modelling various complex pit slope conditions and estimating the failure mechanisms' occurrence. The crucial part of the method is that it is divided into separate elements assigned by a stress-strain relation. The elements hence demonstrate and describe the way the material behaves. Fundamental models such as Young's modulus and Poisson's ratio may serve as a simplified elastic model. The more usual failure criterion for rock masses is the Hoek-Brown criterion, especially in hard rocks (Martin & Stacey, 2018). The Hoek-Brown failure criteria, however, is seldom implemented directly in numerical models. In addition, recent numerical modelling case studies (Frankovska et al, 2015; Khaburi & Mortazavi, 2019; Read & Stacey, 2009) prefer Mohr-Coulomb fit instead of the Hoek-Brown parameters for the computation. Depending on the material being either isotropic or anisotropic, different models can be used. The study of Frankovska et al (2015) shows that the Mohr-Coulomb failure criterion performed smaller deformations compared to the jointed rock model. The latter was developed by PLAXIS and is convenient for the modelling of anisotropy. Safety factor-wise, however, the jointed rock model resulted in a higher safety factor (1.83) in contrast to the Mohr-Coulomb criterion (1.68). Isotropic materials may be modelled with relative ease using simply the material's elastic parameters (Young's modulus and Poisson's ratio). The most often used models for rock masses are those based on linear elastic/perfectly plastic stress-strain relations (Martin & Stacey, 2018). The shear stress that an element can withstand is often modelled using the Mohr-Coulomb strength criteria. Strictly speaking, the tensile strength can only be as high as what has been stipulated. Based on this concept, the rock material displays isotropic behavior. While Mohr-Coulomb strength parameters are used in the presented models, the more usual failure criteria for rock masses is the Hoek-Brown criterion, especially in hard rocks. For particular confining stresses or variations of confining stresses, the Hoek-Brown criteria have more often been employed indirectly in numerical calculations by locating comparable Mohr-Coulomb shear strength parameters that yield a failure surface tangent to the Hoek-Brown failure criterion. Traditional Mohr-Coulomb type constitutive relations make use of the tangent Mohr-Coulomb parameters, which may or may not be updated in the course of investigations. The Hoek- Brown failure

criteria, on the other hand, is often not relevant to weak rocks. Numerical models answer for stresses and displacements simultaneously, and they may keep solving even if certain portions of the model fail. Specifically, the constitutive relations of plasticity need a flow rule that provides a connection between the parts of the strain rate at failure.

2.5.1. Classification

Most rock mechanics modelling studies and literature (Jing & Hudson, 2002; Read & Stacey, 2009; Martin & Stacey, 2017) commonly classify major numerical modeling methods into continuum and discontinuum models. The principal difference among these methods is in the assumption of material being whether continuous or discontinuous, respectively. Continuum models refer to the material as continuous and employ finite element codes that are nowadays integrated into RS2, RS3, FLAC2D, FLAC3D, UDEC, and ABAQUS, as illustrated in Table 1. If major structural features are present, they are simply defined as the interfaces of intertwining continuum materials. Discontinuum methods, on the other hand, treat the material with discontinuities such as faults and joints. Opposite to the finite element code, discontinuum methods utilize discrete elements. The discrete elements are designed to hold numerous discontinuities within its memory allocation system. In the practice, nevertheless, significant major features are considered only. Thus, minor faults or joints that do not really impact the material behavior are not taken into the account. The level of criticality of each individual discontinuity for the model can be determined by the probability of it triggering various failure mechanisms. As a result, a small portion of discontinuities ends up being incorporated into the numerical calculation.

Table 1. Comparison of different codes used for numerical modelling (Martin & Stacey, 2018)

		FLAC FLAC3D	UDEC 3DEC	RS2 (Phase^2) RS^3	Abaqus
Formulation		Finite difference	Finite difference	Finite element	Finite Element
		Continuum	Discontinuum	Continuum	Continuum
		Large deformation	Large deformation	Small deformation	Large deformation
Capabilities	Built-in Material models for weak rock	Mohr–Coulomb, cam-clay, ubiquitous-joint Mohr–Coulomb with cap, softening/hardening cap models	Mohr–Coulomb, cam-clay, ubiquitous-joint	Mohr–Coulomb, cam-clay, anisotropic jointed material, Mohr–Coulomb with cap, softening/hardening cap models	Mohr–Coulomb, jointed material model (similar to ubiquitous-joint)
	Faults	Limited number of faults modelled as discrete interfaces	Multiple faults and joint sets modelled as discrete interfaces	Faults modelled with joint elements (*RS2* only)	Faults modelled as 'cohesive' elements
	Flow models	Porous media Steady-state Transient	Joint only Steady-state Transient	Porous media Steady-state Transient	Porous media Steady-state Transient
	Safety Factor	Automatic via shear strength reduction	Automatic via shear strength reduction	Automatic via shear strength reduction	Manual
Features		Built-in scripting language User-defined material models	Built-in scripting language User-defined material models	User-defined material models	User-defined material models

2.5.2. Input Parameters

The parameters are fed to the numerical calculations and play the governing role in the analysis. It is important to identify and include sufficient laboratory and field monitoring data. The parameters comprised in the analysis may alter depending on the type of numerical modelling and objectives of the research. Typically, two-dimensional finite element and finite difference methods require rock mass parameters such as friction angle, cohesion (c), deformation modulus (E), Poisson's ratio (v), density, and saturated density of the soil (Frankosvka, 2015; Khaburi & Mortazavi, 2019; Read & Stacey, 2009). In regard to the base values, the parameters can be adjusted afterward to run a sensitivity analysis and evaluate the impact of each individual component on the rock slope deformation.

2.5.3. Finite Element and Finite-Difference Methods

The finite element method (FE) is one of the most extensively used numerical methods in the STEM disciplines (Read & Stacey, 2009; Rao, 2018; Jing & Hudson, 2015; Zienkiewicz & Taylor, 2014; Cook et al, 2001). In terms of history, from its inception in the early 1960s, a significant amount of the FE design process has been dedicated to issues in rock mechanics (Jing & Hudson, 2015). This is due to it being the initial numerical technique that could account for non-linear deformability (primarily plasticity), complicated boundary conditions, in-situ loads, and gravity. It was developed in the late 1960s and the beginning of the 1970s when conventional finite difference methods (FDM) using regular grids failed to meet these prerequisites for rock mechanics issues. These benefits allowed it to function better than typical FDM. In its original sense, FE is described as an approximation to continuum problems such that a finite number of elements make up the continuum, and a finite number of parameters define their behavior (Zienkiewicz & Taylor, 2014). Deformation analysis instead of stability analysis was the focus of Duncan's (1996) evaluation of FE analysis of slopes, but he did call attention to some seminal early papers in which elastoplastic soil models have been used to evaluate stability. With cohesion and friction angle in mind, Zienkiewicz et al (1975) found an excellent correlation with slip circle solutions. When comparing the charts of Bishop & Morgenstern with those of Griffiths (2001), it is clear that the latter provides more accurate results for a broader range of soil properties and geometrical conditions. The FE method has since been used for slope stability analysis, which has increased the community's trust in it. In fact, Griffin’s study with Lane (2001) provided an advanced representation of FE convergence and mesh deformation for soil mechanics and slope stability (see Fig. 4). Despite the fact that Duncan (1996) acknowledges FE's potential for better graphical results and reporting, he warns against presuming artificial accuracy given the wide range of input parameters.

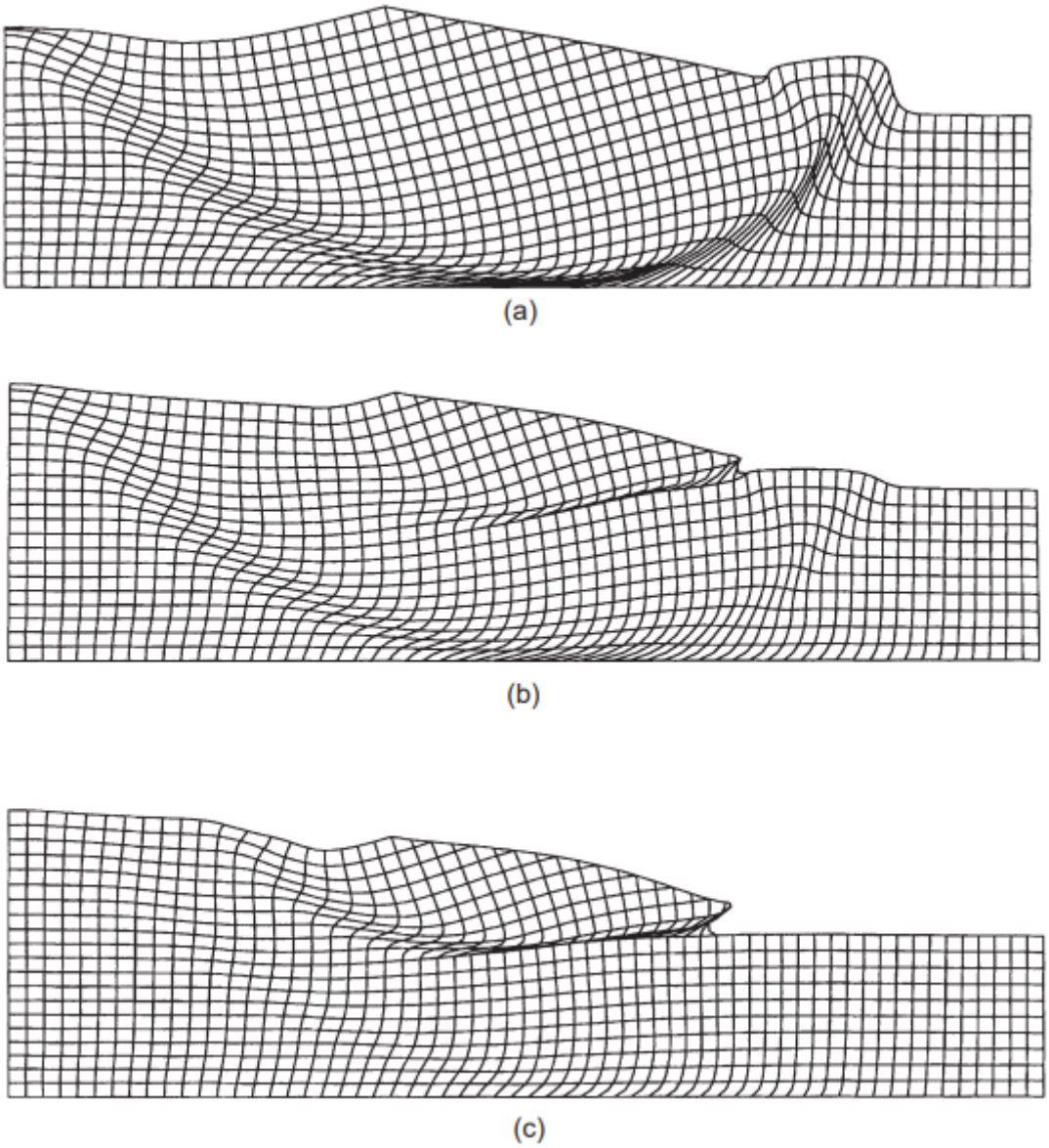

Figure 4. Deformed meshes at failure corresponding to the unconverged solution for three different cohesion ratios between soil and foundation layer (Griffiths & Lane)

In practice, FE and FDM models usually display higher horizontal deformations toward the toe of the rock slope. Such a trend is justified by the excavation-induced shear and compressive stresses. There is a strong link between these induced stresses and major deformation mechanisms (Khaburi & Mortazavi, 2019). Therefore, the sensible approach for the monitoring may require including more monitoring points near the toe zone. Indeed, most two-dimensional

numerical modelling techniques assume only a horizontal displacement close to the toe of the slope. As Read & Stacey (2009) explain, such a boundary condition is mechanically correct given infinitely long slopes. That condition appropriately suits the concept of two-dimensional modelling. The reality of the slope stability problems, however, as the authors suggest, does not always meet this condition. The problem is inherent to three-dimensional modelling, too. Thus, numerical modelling often requires a careful approach to making assumptions as they may have an influence of various extents on the final results. In this regard, both Matthews et al (2014) and Puzrin et al (2010) address the significance of input variables on the ensuing result. In particular, the study on Nicoll Highway Collapse (Whittle, A.J., Davies, R.V., 2006) in Singapore shows that even the slightest falsely estimated or assumed calculations may result in severe accidents. As it turns out, the shear strength of the marine clays might have been overestimated due to the inaccurately assumed effective stress strength parameters (e.g., cohesion, friction angle) for the display of the material The papers may come highly relevant for the thesis, as they emphasize the importance of inserting the correct input data fed to the analysis of the Bozshakol mine as well.

2.5.4. The Scale of the Project

Depending on the scale of the analysis, either two-dimensional or three-dimensional monitoring can be utilized. 2D models are often simpler and may not require as extremely large resources and high computing capacity as 3D ones do. 3D models, nonetheless, provide a wider and more realistic representation of the actual pit given the longer time frame. Although 3D studies were not often undertaken before the advent of modern personal computers, such procedures are now commonplace. As Read & Stacey (2009) point out in their guidelines, pit stability problems are indeed three-dimensional and two-dimensional numerical models may not appropriately evaluate the external stresses flowing all around the pit. Despite the above, many evaluations of slope designs are performed as if the slope were a plane strain in a 2D geometry consisting of a single slice over an infinite length slope (Martin & Stacey, 2018). What this means is it assumes that the radii of the toe and crest are both infinite. This is not the case in the actual world, especially in open-pit mining where the radii of curvature may have a major impact on

safe slope angles. Lack of lateral restriction in convex 'nose' geometries in pit walls might compromise structural integrity. Because of the lateral constraint supplied by the material on each side of a possible failure in a concave slope, they are often more stable than plane-strain slopes. Therefore, there is a shift toward more 3D assessments to more accurately evaluate the stability of complicated geometries, particularly in more brittle materials. There is a high chance that a two-dimensional numerical model with a constant stress assumption will overestimate the stress flowing in a horizontal manner. In contrast to the rising trend of using 3D models, the project will use 2D models. This is rationalized by the limited temporal dimension and computing capabilities.

2.5.5. Advantages of Numerical Modelling and Finite Elements

- The shape and location of the failure surface are not assumed in advance. As the soil mass fails, it does so "naturally" through the areas where the shear strength of the soil is insufficient to withstand the applied forces (Griffiths & Lane, 2001).
- As the FE method does not include slices, no assumptions concerning slice side forces are required. The global equilibrium is maintained until 'failure' is attained using the FE approach.
- The FE solutions will reveal deformations at operational stress levels if accurate soil compressibility data is supplied. The FE technique can track all stages of failure, from first cracking to complete shear failure.
- Numerical modelling represents the material behavior by simulating the elements that are assigned a stress-strain relation. The number of elements comprised in the model is numerous and it affects the accuracy of the simulation. For example, the more the elements can be numerically calculated (given the appropriate mesh), the more accurate representation of the stress levels is anticipated to be obtained.
- Another advantage numerical modelling provides is the opportunity of simulating upcoming production phases and the subsequent change in the stress zones and slope

deformation (Khaburi & Mortazavi, 2019; Read & Stacey, 2009; Kaczmarek & Popielski, 2019). This allows the estimation of relations between initial stress conditions before the mining and after each simulated production stage. In the process, it allows the simulation of shear failure modes and possible brittle rock failures. The necessity of evaluating the stress changes throughout the mining and excavation sequence becomes more apparent as considerable changes take place on the mining site as the mining life cycle passes. Whether it is 20 or 30 years, the changes are anticipated to occur as the pit deepens and thereby it becomes critical to assess them appropriately to monitor possible failure modes (Khaburi & Mortazavi, 2019). Similar to the objectives of the thesis research, it is very important to evaluate the stress changes at a global scale.

- Numerical modelling makes a convenient investigation of the influence of various parameters on the stress level. In so-called sensitivity or parametric analysis, the impact of parameters such as slope wall angle, groundwater level, shear strength, cohesion, and friction angle can be thoroughly investigated and analyzed (Khaburi & Mortazavi, 2019). These are, indeed, the fundamental parameters considered in the computation process. Additionally, the influence of secondary aspects such as a layer of reduced input parameters, the span of the weaker soil layer, strength anisotropy, structural discontinuity at the slope base, and slope soil interaction with rainwater can be examined (Kaczmarek & Popielski, 2019). Examining the effect of groundwater level change would be particularly interesting taking into account that the Bozshakol open-pit mine is experiencing a large amount of groundwater underneath. By introducing the changes in the parameters, different scenarios are generated. These scenarios are then compared to the base case, making it convenient to analyze the influence of each individual parameter on slope stability. An increase in cohesion by 15% under a controlled pit slope angle, for example, results in higher displacement values. Decreasing by 15%, conversely, results in less displacement. In regard to this aspect of the numerical modelling, the thesis work is expected to leverage a similar parametric analysis for appropriate analysis of the Bozshakol open-pit mine.

- Numerical modelling has a lot of advantages over the limit equilibrium and analytical techniques. The limit equilibrium solution merely identifies the commencement of failure, while the numerical solution takes into account the influence of stress redistribution and increasing failure once motion has been commenced (Chiwaye & Stacey, 2010). When it comes to understanding the complicated factors that lead to rock mass breakdown, LE approaches are too simple. Slope stability is affected by a number of factors that are not taken into account in an LE analysis, such as the dilation angle and the horizontal-to-vertical stress ratio (k ratio). More stability than would be predicted by an LE analysis seems to be implied by these characteristics. This implies that the estimations of stability (both FOS and POF) generated by LE approaches are often on the low side. As a result, numerical models are superior resources for calculating the surfaces/volumes of failure for slope failures.
- The absolute majority of the papers appraise the numerical modelling method as the most effective and advanced technique used for modern slope stability analysis, albeit the complexities involved in this time-consuming process. Numerical modelling as a whole has fewer limitations compared to empirical, limit equilibrium, and kinematic approaches. Mostly, only the insufficient amount of data and complicated interface restrain the companies from using this advanced method. In fact, some even claim that the aforementioned FE is not that sophisticated and can be easily used given enough geotechnical monitoring data.

2.5.6. Limitations of Numerical Modelling and Finite Elements

As opposed to the listed multiple advantages above, most literature overlook the specific drawbacks of the numerical calculations. For example, even the highly relevant papers of Read & Stacey (2009), Martin & Stacey (2018), Liu et al (2015), Griffiths & Lane (2001) describe the disadvantages of utilizing numerical tools quite subtly and mostly lack the details. Wiles (2005), on the other hand, point to the low-predictability and high risks associated with the miscalculation of input variables. These were the same reasons that lead to the Nicoll Highway

Collapse that was hence thoroughly studied by Whittle & Davies (2006). Perhaps, such a misinterpretation and improper estimation of inputs are not the disadvantages of numerical modelling itself. This is, rather, a mistake of human nature and can be gradually fixed once appropriate treatment is found. In addition, Wiles (2005) strongly advices to keep the model and geometry as simple as possible given the risks and uncertainties linked to the complexity of some projects. This kind of recommendation may come highly relevant as the Bozshakol copper mine also has intricate geometry and many materials to model. Some of the papers also highlight downsides of the SSR, which is not necessarily applied only for numerical methods. SSR has a broader use in other slope stability tools, including limit equilibrium calculations. Liu et al (2015) shortly mention the inability of SSR to detect other slip surfaces in the model.

3. METHODOLOGY

3.1. Bozshakol Copper Mine

The Bozshakol site geology has an intrinsically complex structure and consists of multiple geotechnical domains accordingly. The conducted pre-feasibility studies (2009) and feasibility studies (2010) beforehand reveal the presence of weathered, fractured, fresh, intrusive, and sedimentary rocks (see Fig. 5). Later investigations of the geology display the occurrence of clay (I, II classes), saprolite, andesite, gabbro, breccia, granodiorite, diorite, and sedimentary (I, II classes) rocks (see Fig. 6).

The central Bozshakol ore field contains the copper deposit. The geological structure of the Bozshakol deposit region includes Cambrian and Ordovician volcanic sedimentary rocks overlain by siliceous sandy-pebble formations with lenses of Paleogene kaolinite clays and Quaternary clays, loams, sands, sandy loams, and pebbles. Many discontinuous disturbances on the ore field region generate the folded-block structure, magmatic complexes, and ore-metasomatic systems.

Large faults control its block structure and alter the distribution of facies and capabilities, whereas small displacement amplitude disturbances and prolonged fractures complicate block

structure. The long-developing Bozshakol fault (or fault zone) confines ore-bearing intrusive bodies (primarily granitoid dikes) of the deposit. The post-ore West-Mysore fault of the north-eastern strike confines the Bozshakol deposit from the east. From the western lakeshore, the diagonal fault crosses the Bozshakol fault zone at a steep angle. Mysore to the southern South Bozshakol gabbroid massif.

Long-term development is also seen in widely established transverse (north-western, north-north-eastern, and sub-meridian) illnesses. These violations split the deposit into blocks: Central, Eastern, Western, Far Western, with different geological structures, ore mineralization, and intensity. Kyzylkainda and West Bozshakol, West Mysore are the greatest transverse faults.

Fig. 7 presents a framework of structural elements that was employed as part of the feasibility study. This framework was created after the data was interpreted. The frameworks of the structural elements were afterwards tested for conformity with the images of the core. These frameworks are based on the ones that were given by KAZ Minerals. The places where the faults can be found in Fig. 8.

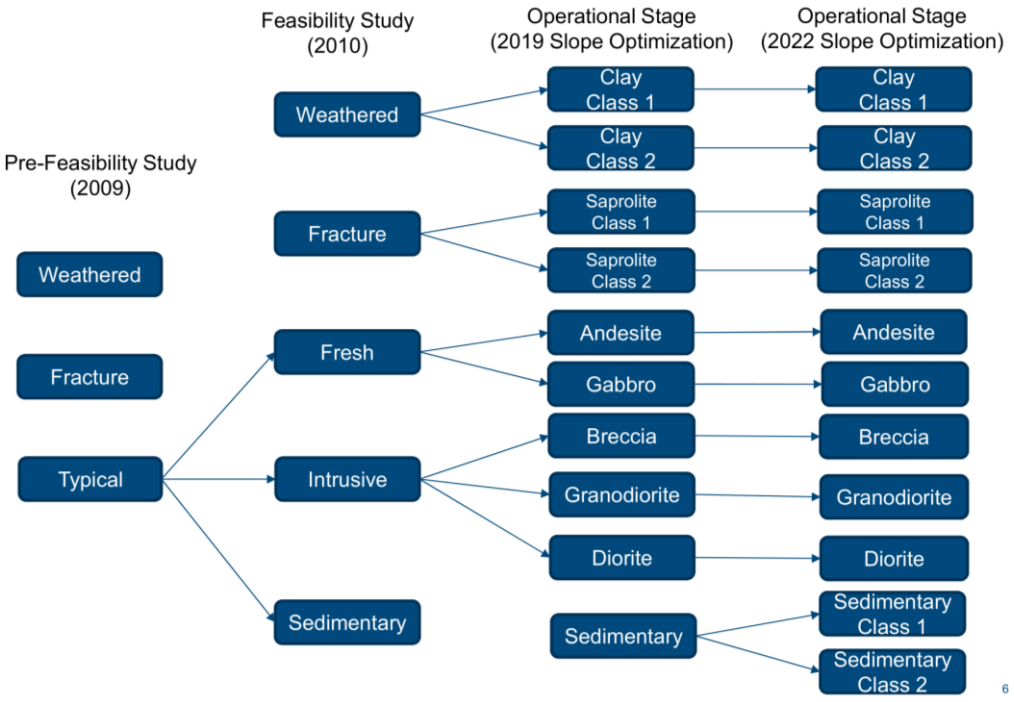

Figure 5. Geotechnical Domains of the Bozshakol Copper Mine (Bozshakol Geotechnical Department)

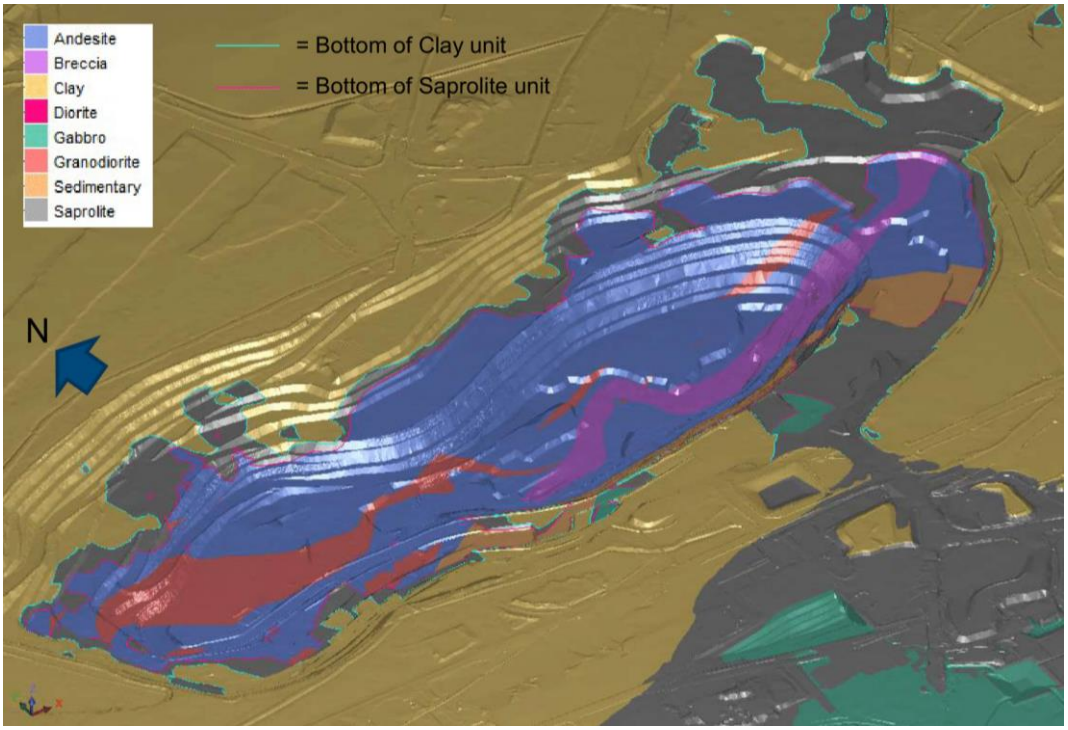

Figure 6. Three-dimensional model of geotechnical domains in the site (Bozshakol Geotechnical Department)

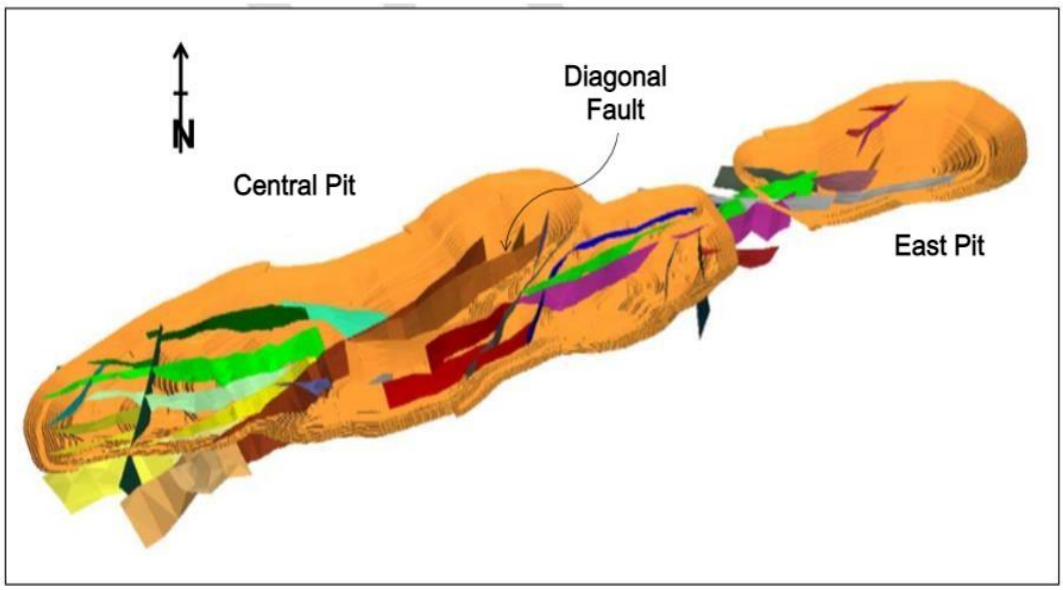

Figure 7. Structural model of the Bozshakol pit (Bozshakol Geotechnical Department)

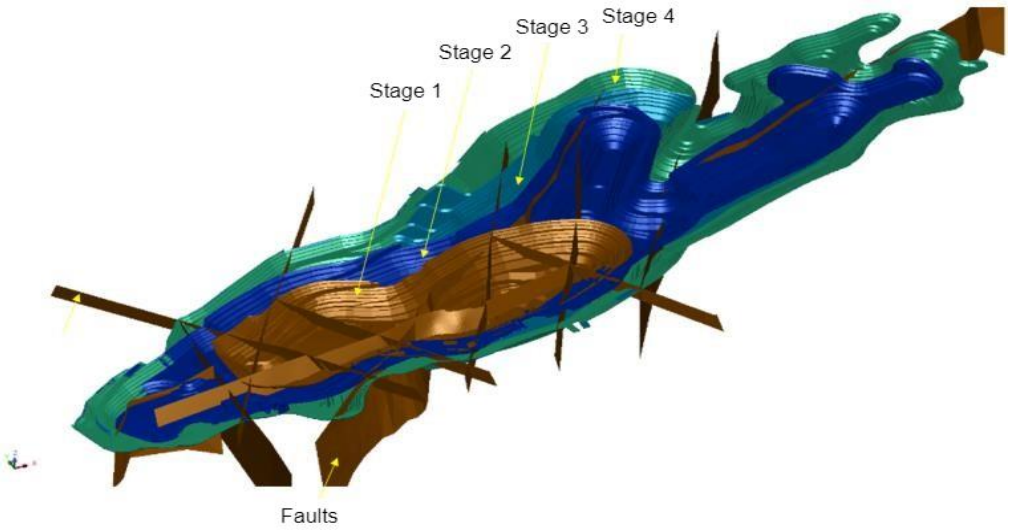

Figure 8. The location of faults in the Bozshakol pit (Bozshakol Geotechnical Department)

3.2. Finite Elements

As mentioned earlier, the paper is heavily focused on FE as its main method to numerically simulate the behavior of the slopes. Although FE itself emerged to the industry in the mid-20th century, it is still the dominant and rigid tool among other numerical methods. The earliest application of the finite element approach was in the study of aeronautical constructions. Yet, the breadth of its theory allows it to be applied to many other geomechanics and engineering boundary value issues.

3.2.1. Theory

In order to get an answer, one must satisfy certain boundary (edge) conditions on the dependent variables or their derivatives, thus this type of problem is known as a boundary value problem. There are three main types of boundary value issues that may be solved using the finite element method: (1) problems of equilibrium, steady state, or independency in time; (2) eigenvalue problems; and (3) propagation or transient problems.

Table 2. The main steps in finite element modelling for boundary condition problems (Rao, 2018)

N	General Steps in FE	Description
1	Structure Discretization	For the finite element approach to work, the structure or solution area must first be broken down into smaller pieces, known as elements. For this reason, appropriate finite elements must be used to model the structure. It is up to the designer to determine the element count, variety, dimensions, and layout.
2	Building a displacement model	We assume some suitable solution within an element to approximate the unknown solution, as it is impossible to precisely predict the displacement solution of a complicated system under any given loading. From a computational aspect, the assumed solution needs to be straightforward, but it still needs to converge as expected. The solution or interpolation model is typically expressed as a polynomial
3	Stress stiffness matrices and loading vectors	It is expected that equilibrium conditions or a sufficient variational approach will be used to determine the stiffness matrix $[K^{(e)}]$ and the load vector $\vec{P}^{(e)}$ of element from the postulated displacement model.
4	Obtaining the general equilibrium equation	Boundary circumstances necessitate adjustments to the overall equilibrium equations. When boundary conditions are included, the equilibrium equations become $\underline{[K]}[\mathrm{D}] = \underline{\overrightarrow{[F]}}$ (1)

		The vector $\underline{\overrightarrow{[F]}}$ is highly useful for solving linear equations. The solution to a nonlinear issue, however, requires a series of iterations in which the stiffness matrix [K] and/or the loading vector [P] are changed.
5	Nodal displacements calculation	Due to the fact that the structure is made up of a number of finite elements, it is necessary to assemble the stiffness matrices and load vectors for each element in a way that makes sense, and then express the overall equilibrium equations as $$\underline{[K]}[\mathrm{D}] = \underline{\overrightarrow{[F]}} \quad (2)$$ where [K] is the reassembled stiffness matrix, [D] is the vector of nodal displacements, and $\underline{\overrightarrow{[F]}}$ is the vector of nodal forces.
6	Element strains and stress calculation	If necessary, using the appropriate equations of geomechanics, the element strains and stresses can be calculated from the known nodal displacements $\overrightarrow{\Phi}$. To apply the idea to new domains, we must adjust the vocabulary employed in the first six steps. To avoid confusion, we must refer to the structure as a continuum or domain, the displacement as a field variable, the characteristic matrix as the stiffness matrix, and the resultants of the elements as the strains of the elements. The following examples demonstrate the use of the six stages of finite element analysis.

3.2.2. Stress Reduction Technique

To find the stress reduction factor (SRF) or factor of safety value that pushes a slope to its ultimate boundaries of failure, engineers use the Shear Strength Reduction (SSR) technique of Finite Element (FE) slope stability analysis. SRF was implemented late 20^{th} century by Zinkiewicz et al (1975) to model the slope by FE given the multiple materials are present. In that case, shear-stress reduction is applied for all the materials comprised in the model at the same time. As compared to limit equilibrium methods, which are typically used in evaluations of slope stability, the shear-strength reduction approach offers two key benefits. First, the crucial sliding surface is identified automatically; you don't have to worry about deciding in advance whether it will be circular, log spiral, or piecewise linear (Read & Stacey, 2009). Slopes typically have a failure surface geometry that is more intricate than that of circles or regular polygons. And second, translational and rotational equilibrium are automatically satisfied by numerical methods, although this is not always the case with limit equilibrium approaches. Hence, a FoS that is equivalent to or slightly lower than that obtained using limit equilibrium techniques is often established using the shear-strength reduction methodology. In RS2, SRF is automatically set to 1. Critical SRF, on the other hand, is generally the lowest SRF value that results in stress analysis convergence. This is possible with the iterations of the shear strength reduction (SSR). In this paper, SRF is applied to determine the critical SRF.

Most of the literature on SSR assume that slope materials have Mohr-Coulomb strength (Hammah et al, 2004; Read & Stacey, 2009; Zinkiewicz et al, 2014). The most extensively used failure criterion in engineering analysis is the Mohr-Coulomb strength envelope. The uniqueness of this linear failure model lies in the fact that it may be described in a straightforward and explicit fashion in both principal stresses (sigma 1 and sigma 3) and shear-normal stress space.
The Mohr-Coulomb criterion is widely used because of its simplicity, straightforward representation in primary and shear-normal stress space, appropriate description of strength behavior for a wide variety of materials, and easily obtainable parameters.

The equation can be used to calculate the scaled or lowered shear strength of Mohr-Coulomb materials:

$$\frac{t}{F} = \frac{c'}{F} + \frac{tanf'}{F} \tag{3}$$

Alternatively, the equation can be modified as follows:

$$\frac{t}{F} = c* + tanf* \tag{4}$$

where *c** and tan*f** are the reduced Mohr-Coulomb shear-strength properties.

3.3. Geotechnical Data

With the objective of maximizing the control over the pit and mitigating slope-related emergencies efficiently, the site is divided into 8 respective sectors (see Fig. 9). Almost each of the sectors has a unique slope structure and production stages planned. Stage 2, in this regard, is the current stage of production. Based on the assumption of the geotechnical sectors 2 and 6 having a potentially unstable wall and steeper slope angles than any other sectors presented in the datum, a perpendicular two-dimensional slice of this region was specifically chosen for the modeling. The production stages constituent in the sector thus would be from 2 to 6, respectively.

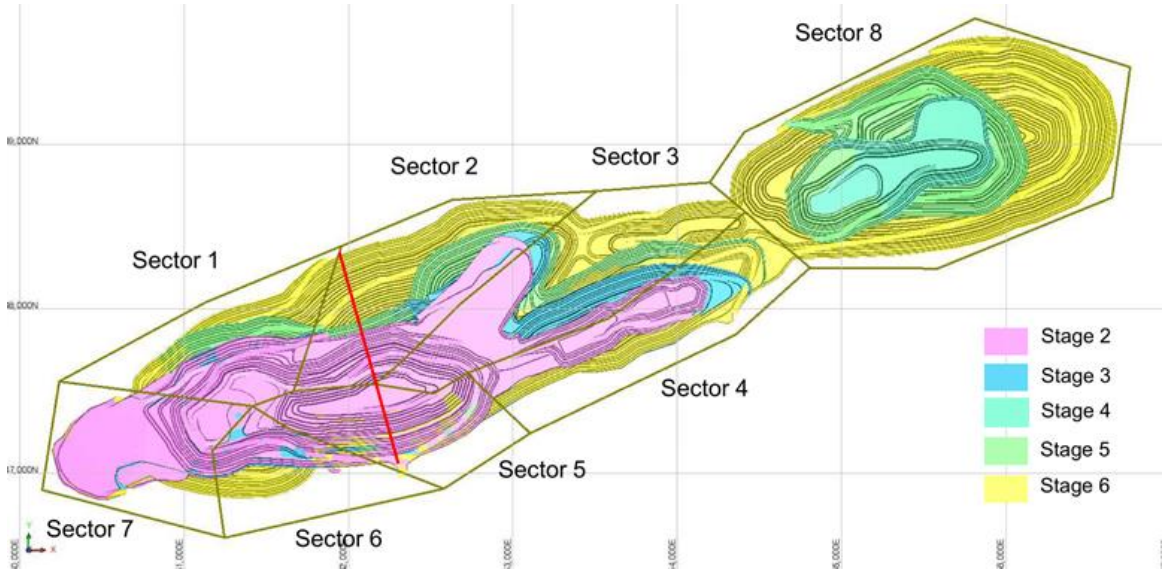

Figure 9. The geotechnical design sectors of KAZ Minerals Bozshakol

(Bozshakol Geotechnical Department)

3.4. Modelling strategy

The modelling strategy is comprised from seven inter-related development steps:

- **Identification of material boundaries.** The boundaries of andesite, breccia, and gabbro are drawn in accordance with the geometries displayed on 2D model (see Fig. 10). This 2D section of the pit is highlighted with the red line in Fig. 9.

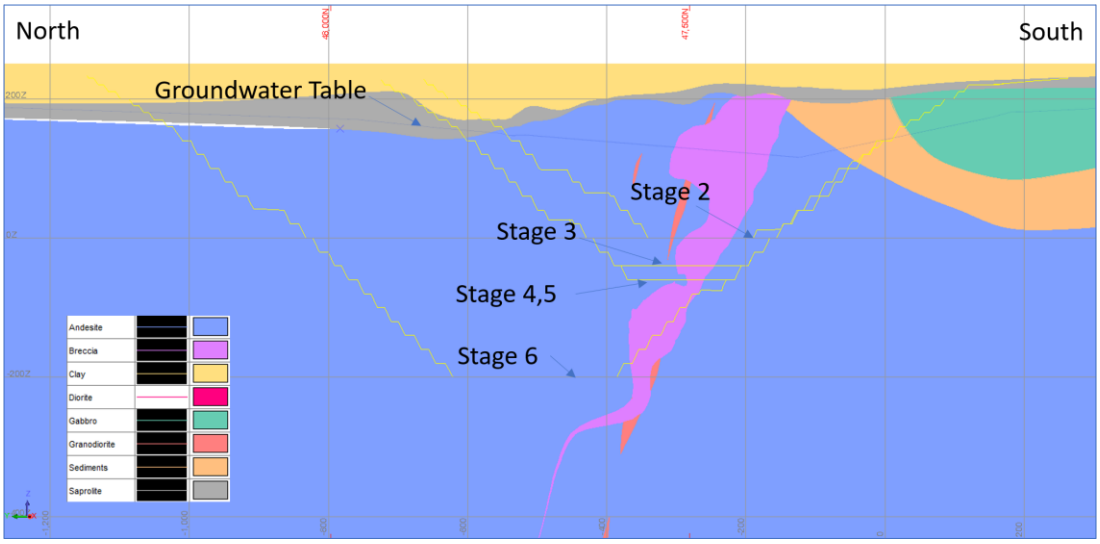

Figure 10. Two-dimensional model of the pit between the sectors 2-6

- **Evaluation of rock mass properties.** Since numerical models require rock mass parameters as their main input data, it is crucial to feed Hoek-Brown classification (or intact rock) parameters to the rock strength analysis. RocScience RocLab is thereby used for the estimation of peak tensile strength, uniaxial compressive strength, elasticity modulus, global strength, cohesion, and friction angle at the rock mass scale.
- **Fitting the geometry of the model.** The modelling strategy using FE suggests the division into 5 consecutive production stages, where stage 0 is an initial pre-production phase solely affected by the in-situ stresses, and stage 6 represents the ultimate limit of the mining. This, in turn, allows us to look at the changes in pit wall displacement field, deformation contours, deformation boundaries, and stress trajectories throughout the lifetime of the mine. In accordance with the original geometry, the constructed 2D model is 1270 meters wide and 720 meters high. Most importantly, however, is to keep the model as simple as possible due to high risks associated with improper evaluations given the complexity of the project. This was, as mentioned, being recommended by several researchers, including Wiles (2006) and Whittle & Davies (2006)
- **Discretion and Mesh.** The mesh, in regard to the size of the model, is uniformly set by triangular elements, resulting in approximately 5000 commutation zones. It is considered to be near-perfect for the model as such a vast number of elements provides

more accurate results. Further use of quadrilateral nodes and an increase in element number is thought to be inconceivable given the redundancy and computational capacities.

- **Staging.** The major contribution of this project is to appropriately model all the production stages of the Bozshakol mine, as illustrated in Fig. 10. This gives an extensive look at the changes in-between the stages given the time dimension. That is, alterations in the displacements, stress levels, and deformation boundaries. Currently, the excavation of Bozshakol is in its second stage.
- **Groundwater, Restrains and Stress Field.** Hydrogeological regimes, including groundwater pressure and surface water flow, may have a substantial detrimental impact on slope stability, and both must be recognized. These features are typically the only ones in a slope design that can be easily altered by human intervention, especially at a large scale (inter-ramp and bigger). Although dewatering and depressurization techniques are normally done with considerable lead time, they require operator commitment to be successful (Read & Stacey, 2009). Thus, it is crucial to identify and characterize the hydrogeological regime at the outset of every project. The groundwater level for this project is the same as in Fig. 10 and Fig. 12.
- **Stress Reduction Factor.** As mentioned in Section 3.2.2, the stress reduction factor can be interpreted as a factor of safety or vice versa. By enabling this technique in RS2, the iterations will start from SRF = 1 and calculate the critical SRF, at which equilibrium is achieved. Critical SRF might show interesting results from the slope on the verge of failure (Hammah et al, 2004). This is why it is important to display different failure scenarios at correspondingly different SRFs (e.g., low, critical, high). SRF, at which slope is in the most stable conditions, is thought to be the convenient factor for safety. For example, in Fig. 11, SRF of 1.15 is presumed to be the maximum FoS that had stable slope (Hammah et al, 2004).

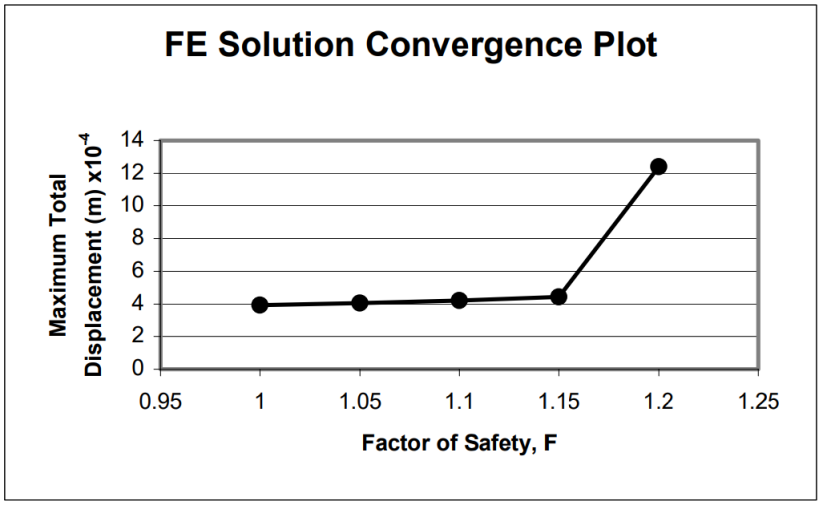

Figure 11. The chart of SRF against peak total displacement field (Hammah et al, 2004)

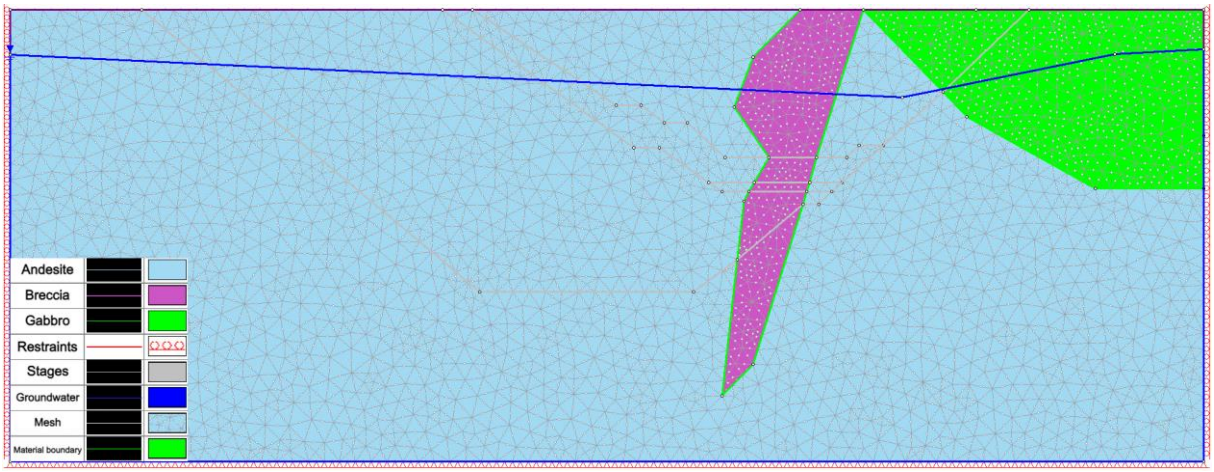

Figure 12. The constructed 2D FE model of the Bozshakol pit using the RS2 code

3.5. Sensitivity Analysis

The sensitivity of the pit to alterations in various parameters might reveal the weaknesses of the slopes. Accordingly, it helps identify the proneness of the wall to failure given these properties change. It can be measured by the deviations in the displacements or deformation conditions once the alterations take place. In practice, however, the rock properties are still the same, and slope angles do not change drastically. The overall angles of the wall are typically predetermined during the preliminary geotechnical design as they play a pivotal role in the production safety. Sensitivity analysis, on the other hand, generally helps understand the effects

of property changes on the basis of real-world case studies. The analysis is conducted on the basis of deviations in the RMR of the andesite (see Table 3). This is due to the fact that andesite is the host rock and covers most of the model.

Table 3. The recorded ranges of RMR of andesite in Bozshakol (KAZ Minerals Bozshakol Data, 2020)

Rock	Categories	RMR	Rock Quality (Bieniawski, 1993)	Change, %
Andesite	Lowest	25	Poor	-55
	Mean	55	Fair	0
	Highest	75	Good	+35

3.6. Input parameters

The input data fed to the FE largely consists of material strength parameters. In spite of KAZ Minerals having the earliest LEM and FE records on crucial parameters such as unit weight, UCS, GSI, intact rock constant, disturbance factor, Poisson's ratio, porosity, and tensile strength, it was our highest priority to calculate the cohesion, elasticity modulus, and friction angle. The intact rock parameters are hence used for the rock mass strength analysis using RocLab program. In that regard, all three rocks comprised within the model are analyzed through Mohr-Coulomb fit.

Table 4. Intact rock material properties used for the modelling
(KAZ Minerals Bozshakol Data, 2020)

Material	Unit weight, γ (MN/m3)	Poisson's ratio, v	Median UCS, σ (MPa)	GSI	Instant Rock Constant (mi)	Disturbance Factor (D)
Andesite	0.029	0.25	48	60	25	0.0 – 0.7
Breccia	0.028	0.26	43	55	19	0.0 – 0.7
Gabbro	0.027	0.24	14	45	15	0.0 – 0.7

4. RESULTS

4.1. Rock Mass Design Parameters

From the Hoek-Brown classification parameters, both the needed Mohr-Coulomb fit and rock mass properties were calculated (see Table 5 and Figs. 13-15). In relation to each other, andesite as a host rock possesses a higher uniaxial compressive strength and elasticity modulus.

Table 5. Rock Mass Properties determined for major geotechnical units of Bozshakol

Rock	Cohesion, *c* (MPa)	Friction Angle, φ (degrees)	Tensile strength, σ (MPa)	UCS, σ (MPa)	Global strength, σ (MPa)	Modulus of deformation, E (MPa)
Andesite	3.32	39.3	-0.07	4.0	14.0	10472
Breccia	2.54	35.1	-0.06	2.6	9.8	7432
Gabbro	0.65	29.6	-0.01	0.4	2.2	2385

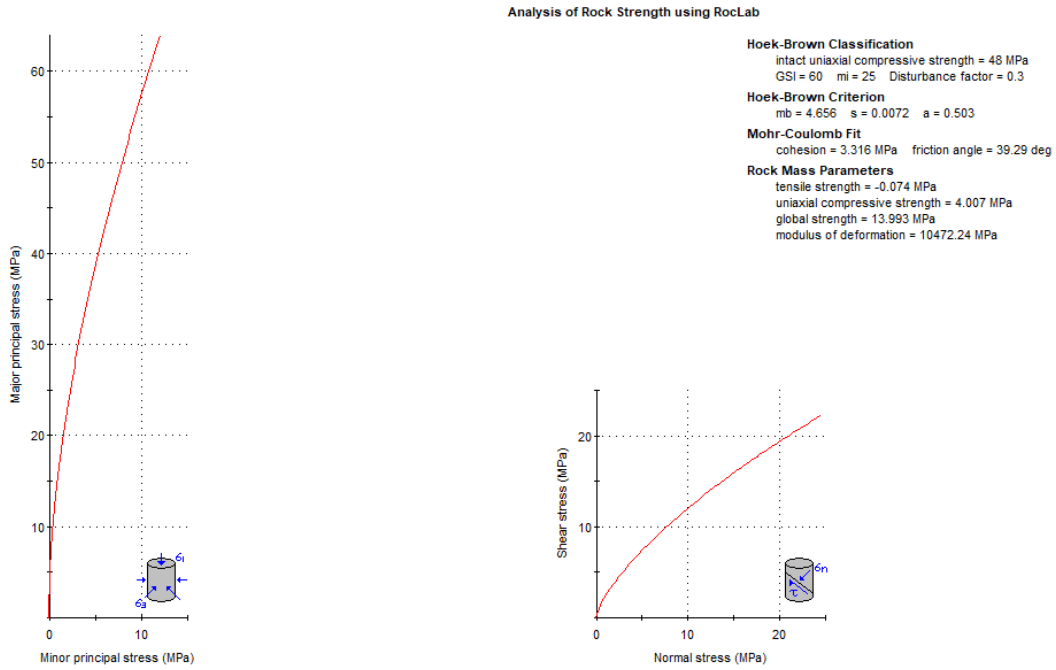

Figure 13. Determination of rock mass design data for the Andesite unit.

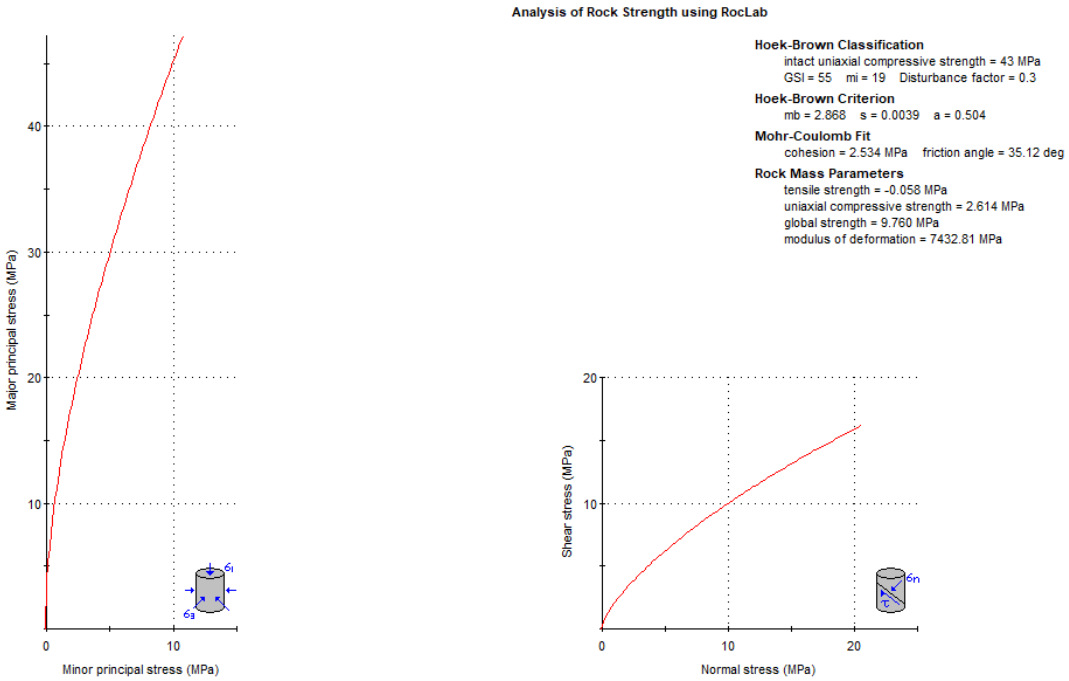

Figure 14. Determination of rock mass design data for the Breccia unit.

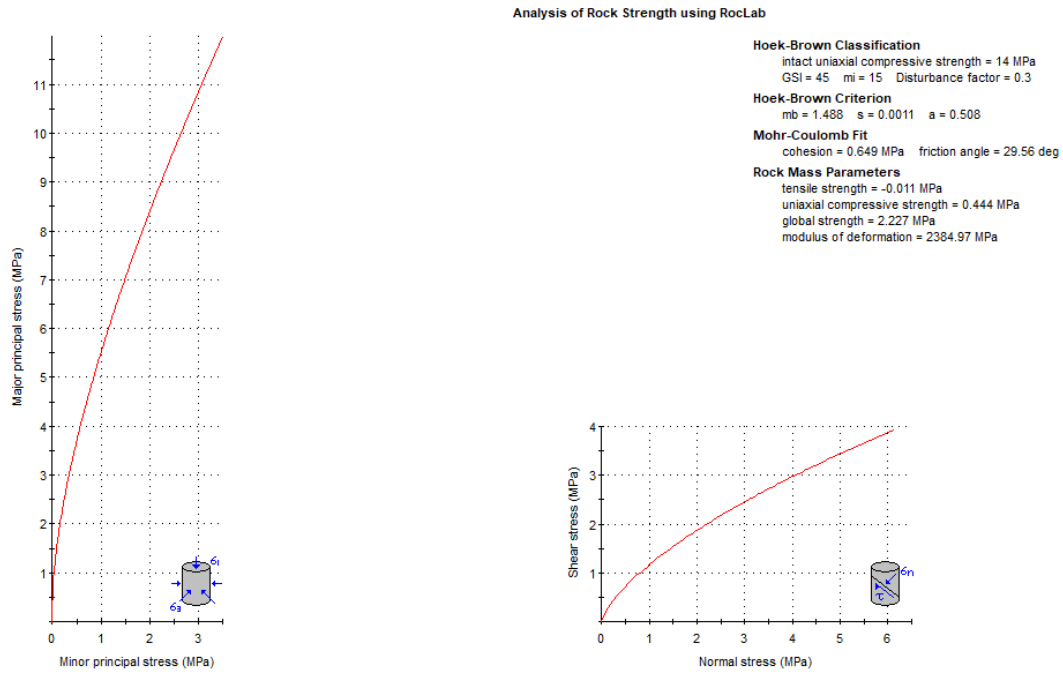

Figure 15. Determination of rock mass design data for the Gabbro unit.

4.2. Numerical Simulation Results

4.2.1. Pre-mining Conditions (Stage 0)

Although analyzing the solid displacements in stage 0 is not highly critical, it is worth noticing that high movements along the breccia-gabbro boundary are present (see Fig. 16). In regard to the total stresses of the model, the principal stresses sigma 1 and sigma 3 are comparatively similar (see Figs. 17-18). The maximum values of principal stress sigma 1 and principal stress sigma 3 reach 21 MPa and 20.81 MPa, respectively.

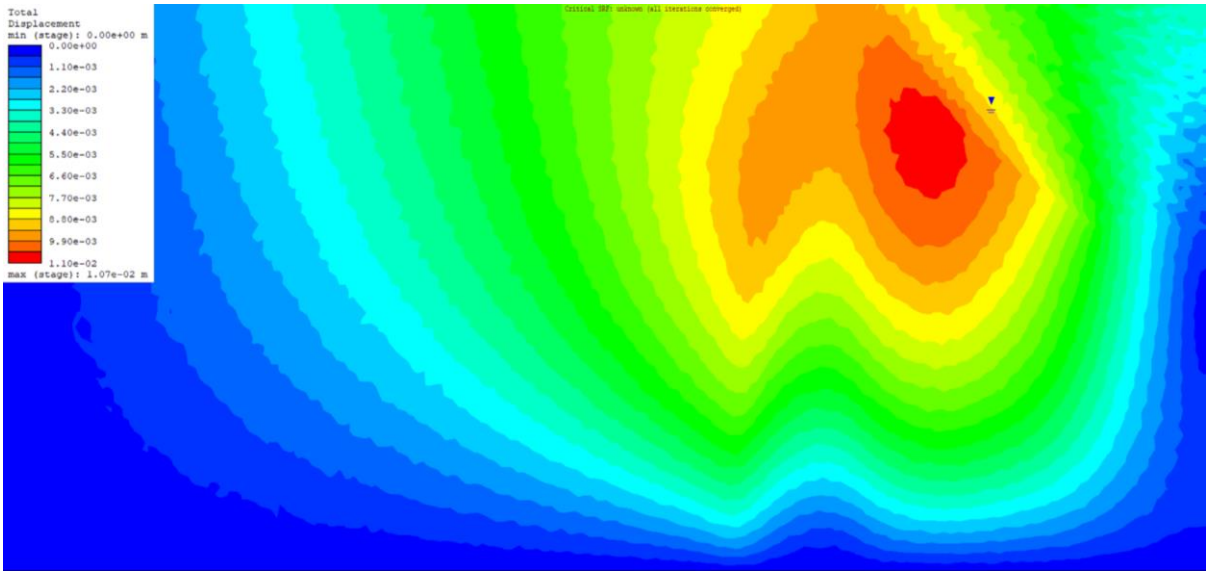

Figure 16. Total displacement field in prior to mining (Production stage 0)

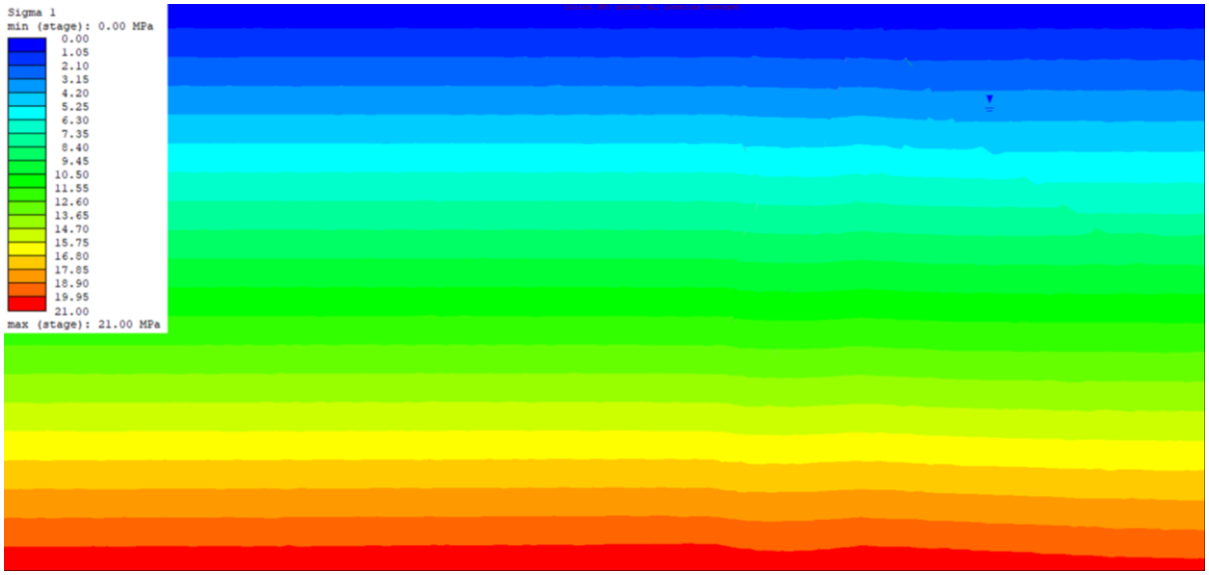

Figure 17. Maximum principal stress (Sigma 1) distribution in production stage 0

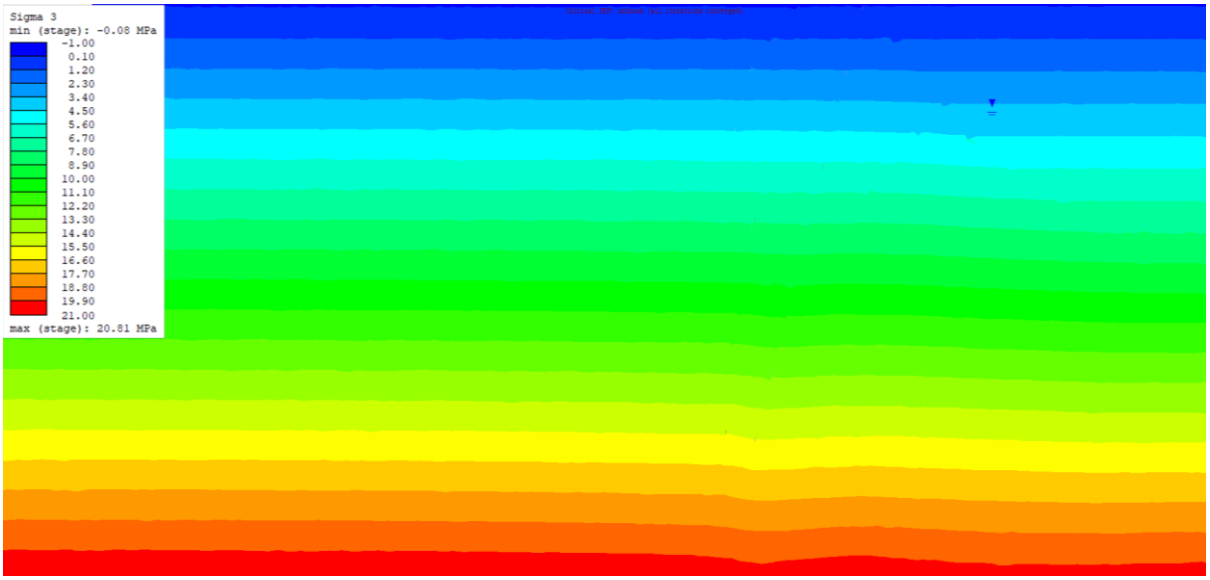

Figure 18. Maximum principal stress (Sigma 3) distribution in production stage 0

4.2.2. Production Stages

By utilizing the stress-strength reduction technique to its maximum, major deformation zones are revealed across the production stages, as illustrated in Figs. 19–22. Critical SRF, in this regard, presented mostly minor displacements. The progression of the deformation scenarios between the low and high SRF values could take place given the time dimension. In other words, stresses could accumulate around the gabbro, which is a weak rock in this model, causing a planar slide.

Stage 2

Given the critical SRF of 2.15, the current production phase of the Bozshakol, as the results of FE display indicate, is prone to a minor deformation in the south (right) wall (see Fig. 19). The vectors perfectly illustrate the downward direction of the solid movement. This deformation zone is situated in the same area as gabbro. A wide range of movements around the bottom and lateral sides of the model show the impacts of mining and excavation. It is worth noticing that a maximum displacement of 0.035 m might indicate the sufficient safety of the south wall. In regard to the remaining zones of the pit, displacements up to 0.025 m are anticipated. The results also imply that the north wall is comparatively safer than the south wall at this moment. However, given the maximum SRF of 2.6, the south wall could be deformed severely with displacements up to 3.3 m. It means that the strength of the rock may diminish with time and stresses start to accumulate. Indeed, the stress levels start to rise near the slopes given the time dimension (see Appendix C).

Stage 3

The scenario of production stage 3 is relatively similar to the one shown in stage 2 (see Fig. 20). It appears that the top-south part of the pit is highly sensitive to large-scale deformation. The mechanism starts with active mining-induced displacements at lower SRF and starts growing around the top-south wall, where the rock strength is greatly reduced and stresses accordingly rise. The solid displacements are predicted to reach a maximum of 0.05 m. It is

relatively greater than that shown in the previous model. The movements are directed towards the bottom of the pit, implying a high probability of downward planar or circular failure.

Stages 4-5

The FE analysis of production stages 4-5 resulted in higher displacements with the maximum equal to 0.07 m as opposed to the previous phase. The bottom of the pit and remaining zones of the south wall show displacements between 0.05 m and 0.07 m. The movement from the both slopes and pit bottom, in that sense, similarly indicates the impact of mining and excavation activities.

Stage 6

The most concerning scenario among all those analyzed might happen in production stage 6, as illustrated in Fig. 22. The maximum displacement of 0.14 m, given the critical SRF of 2.21, is nevertheless manageable. The range of the deformation, however, increased in comparison to the previous production phases. As can be observed, the north (left) wall of the pit is less prone to major deformations even during the ultimate pit excavation.

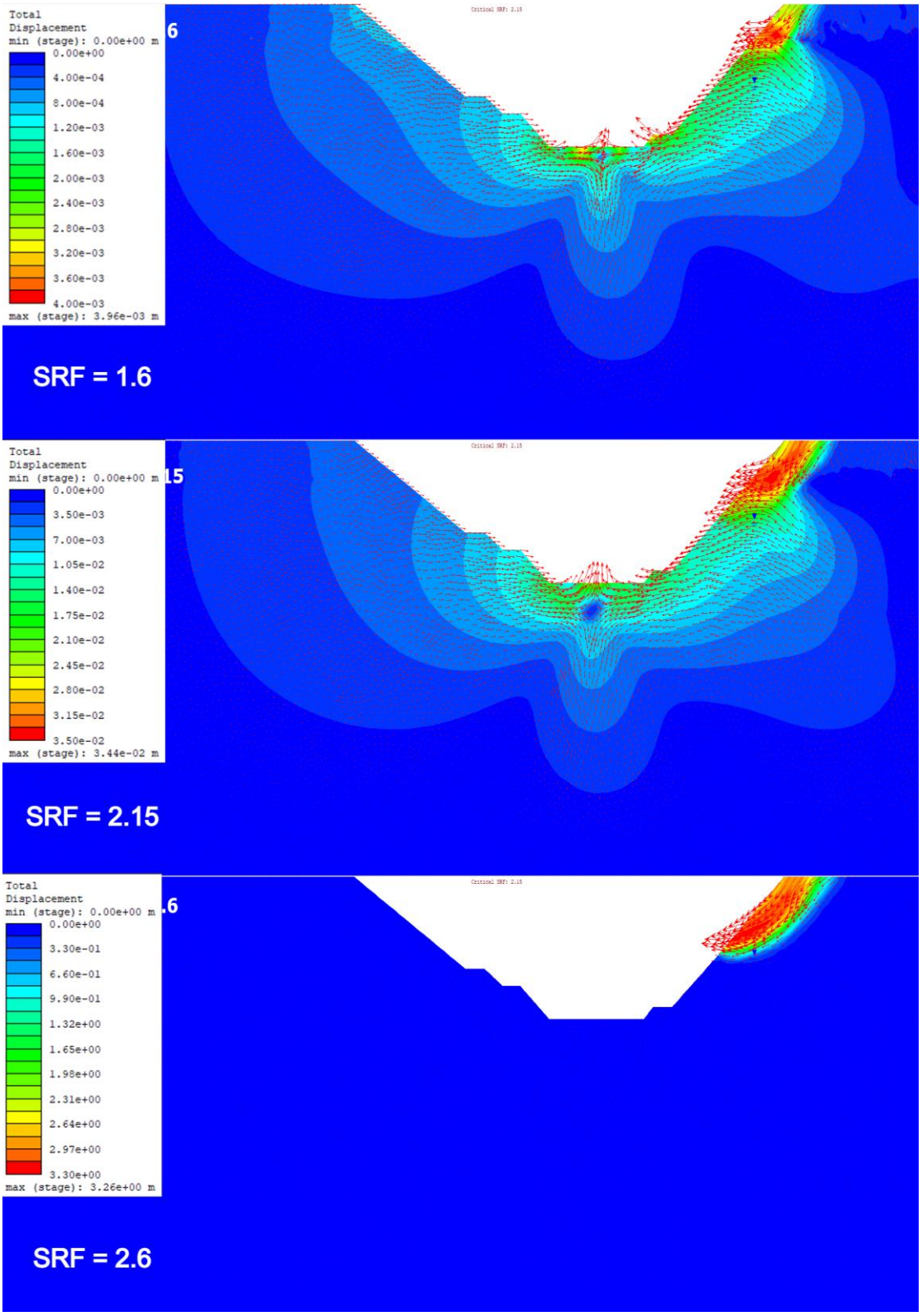

Figure 19. The calculated wall displacement field in production stage 2 (N-S Section).

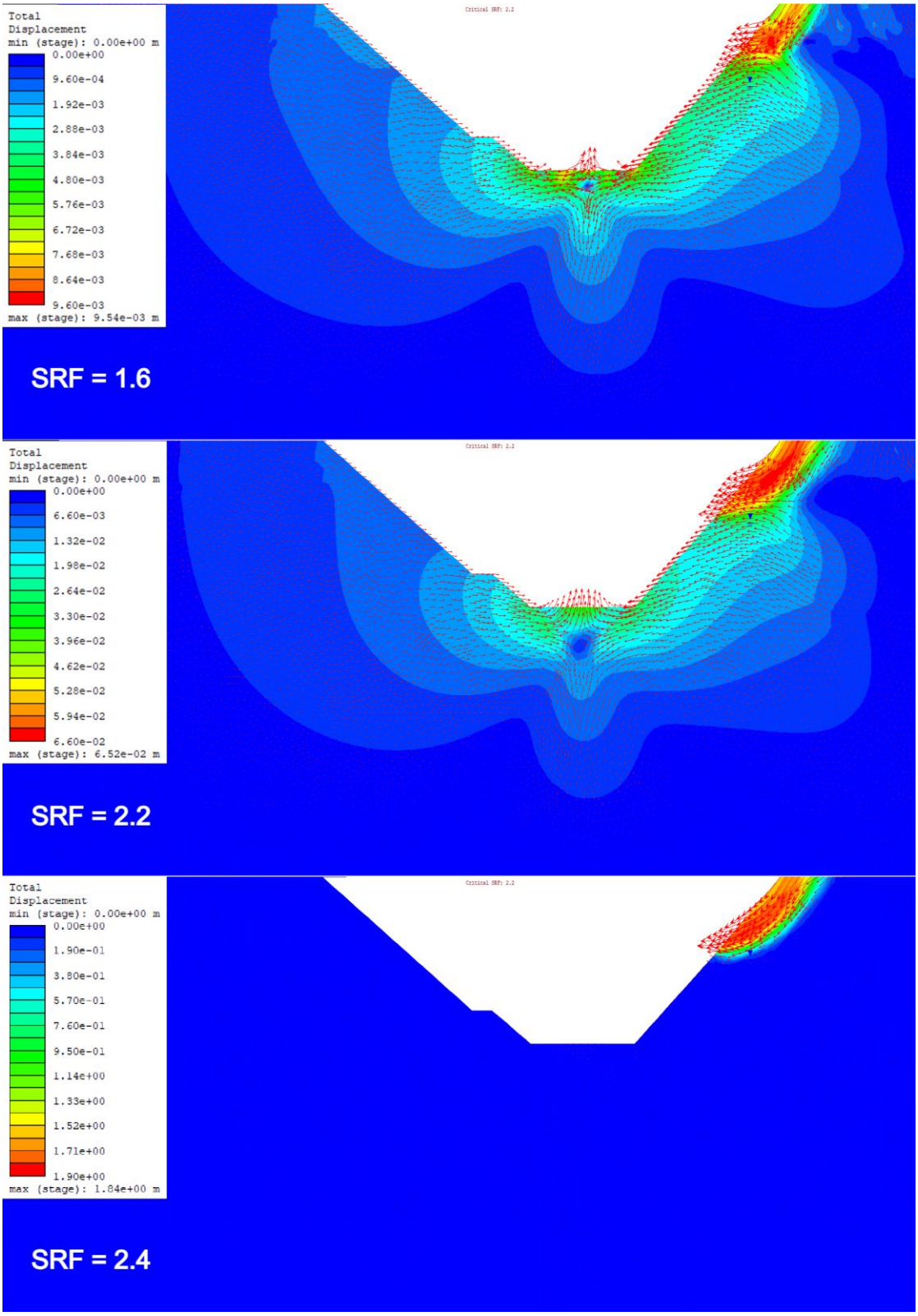

Figure 20. The calculated wall displacement field in production stage 3 (N-S Section).

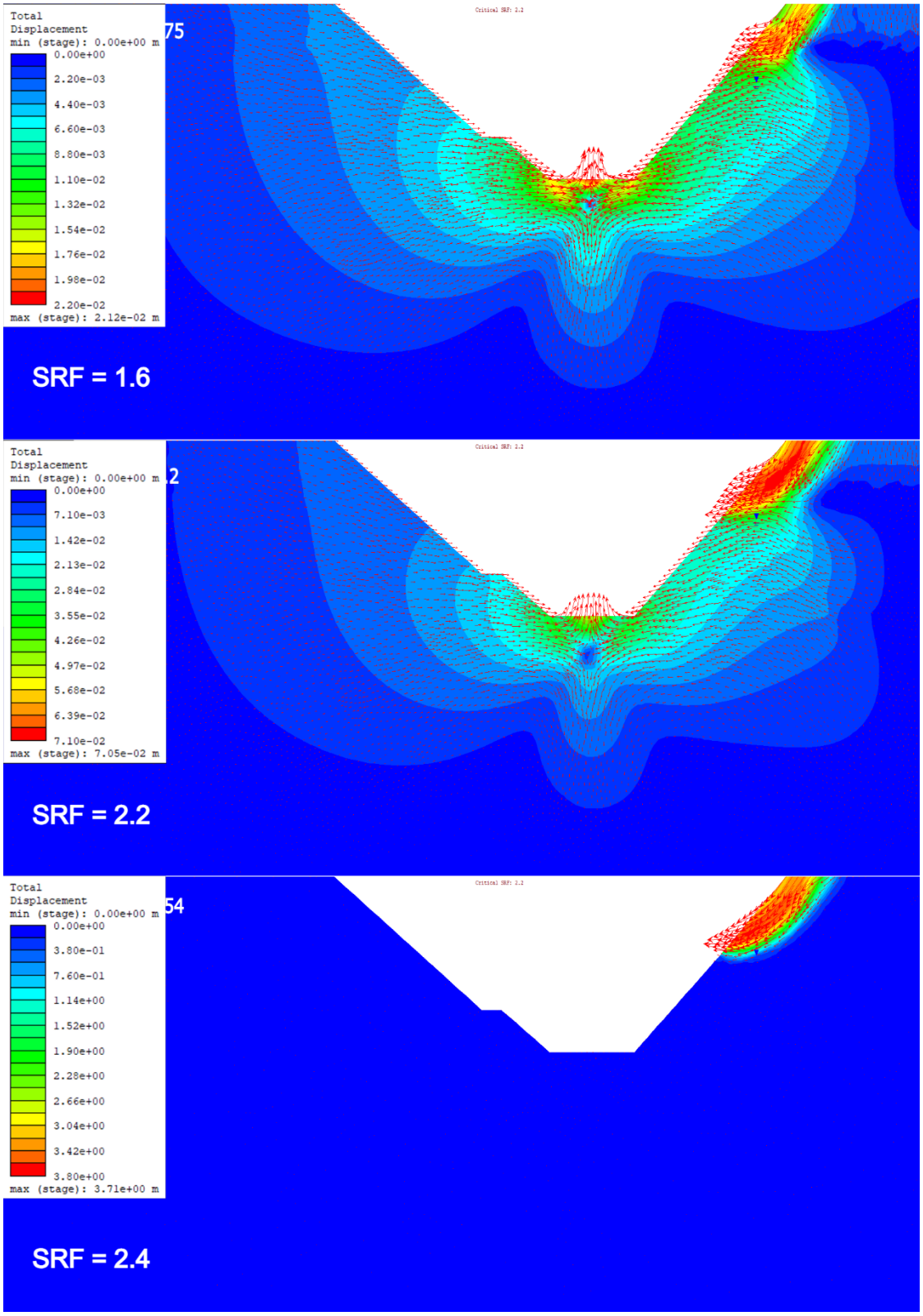

Figure 21. The calculated wall displacement field in production stages 4-5 (N-S Section).

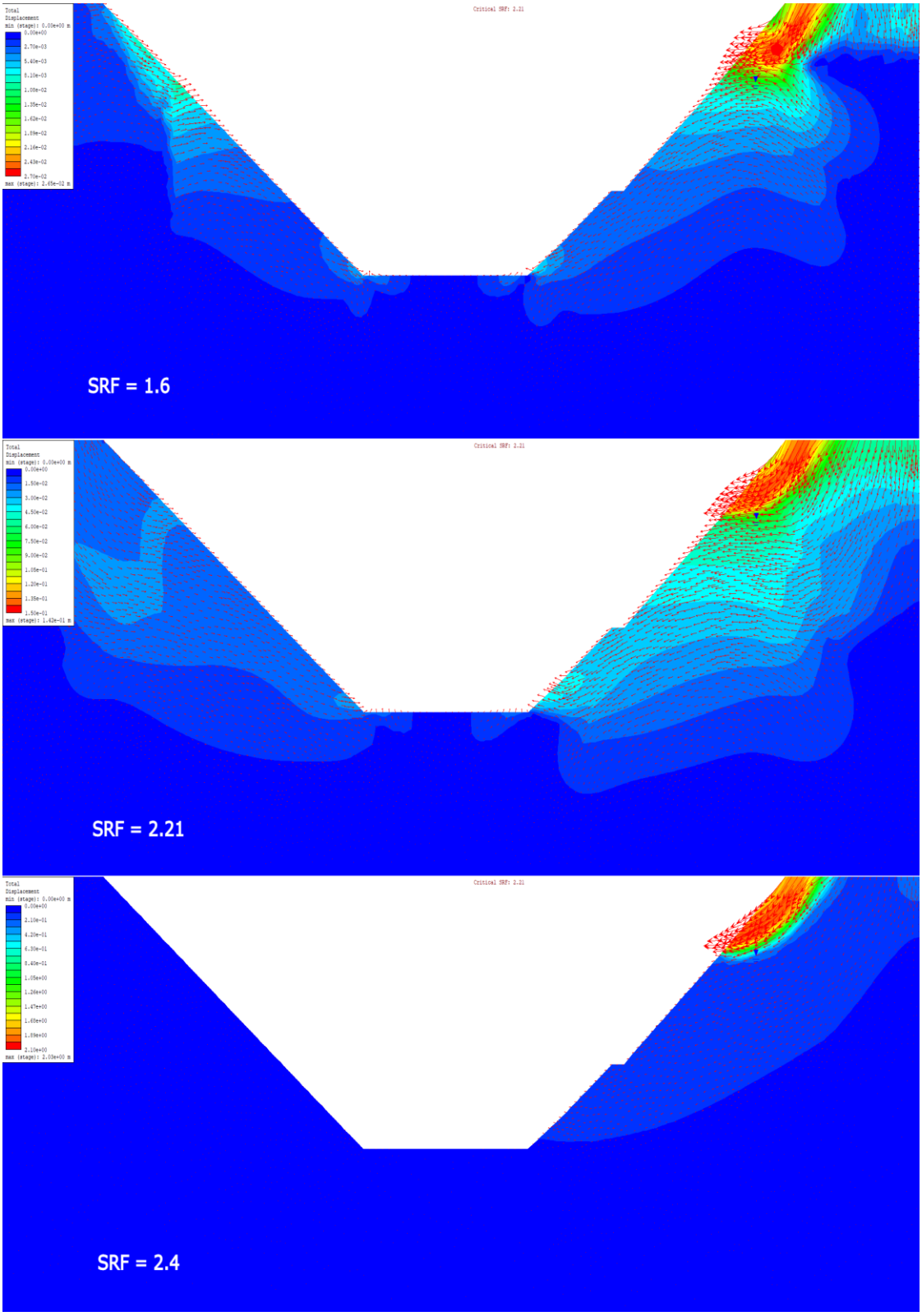

Figure 22. The calculated wall displacement field in production stage 6 (N-S Section).

4.3. Sensitivity Analysis

In accordance with Section 2.5 and Table 3, the sensitivity analysis is conducted with the indicated changes in cohesion, friction angle, and elasticity modulus of andesite. The altered values are presented in Table 6. Also, the sensitivity analysis is applied only on production stage 2, as it already provides a wide look at the deviations from the base value.

Table 6. Altered rock mass parameters of andesite used for the sensitivity analysis

Rock Type	Change, %	Cohesion, *c* (MPa)	Friction Angle, φ (degrees)	Elasticity Modulus, E (MPa)
Andesite	-55	1.5	17.7	4712
	0 (Base Value)	3.3	39.3	10472
	+35	4.5	53.0	14138

4.3.1. Change in Elasticity Modulus

Reduced elasticity modulus

The impact of a reduced Young's modulus is inversely proportional to the solid displacements and deformation area. As the modulus was decreased to 4760 MPa, the displacements increased in magnitude, as illustrated in Fig. 23. In comparison to the base case scenario, the displacements have now reached their maximum of 0.16 m given the critical SRF of 2.21.

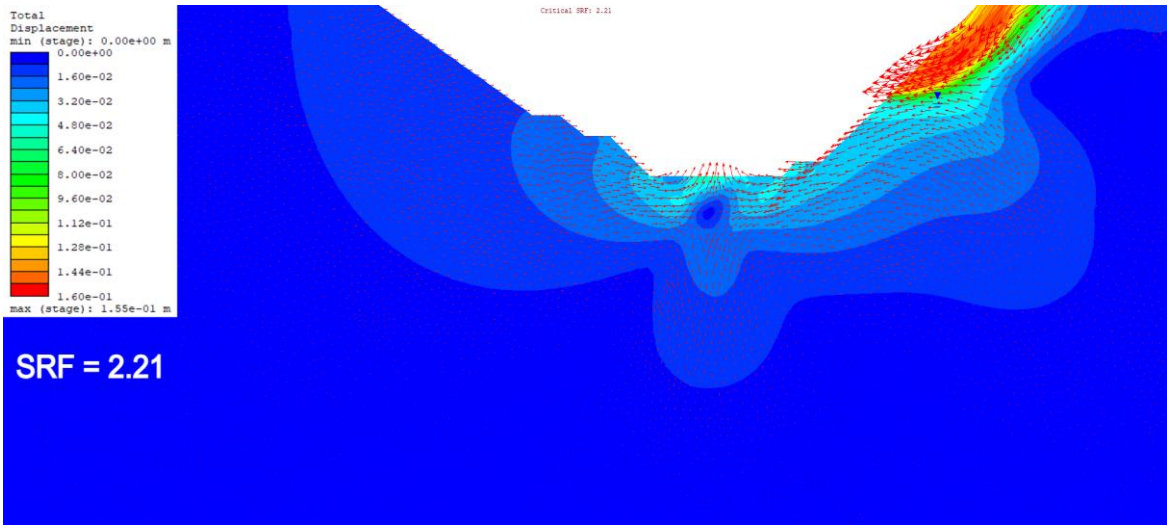

Figure 23. The calculated wall displacement field with reduced elasticity modulus in production stage 2

Increased elasticity modulus

The enhancement of elasticity modulus, as expected, resulted in a decrease in displacements. The reduction of major deformation zones as well as the maximum displacement of 0.018 m at the critical SRF are observed in Fig. 24.

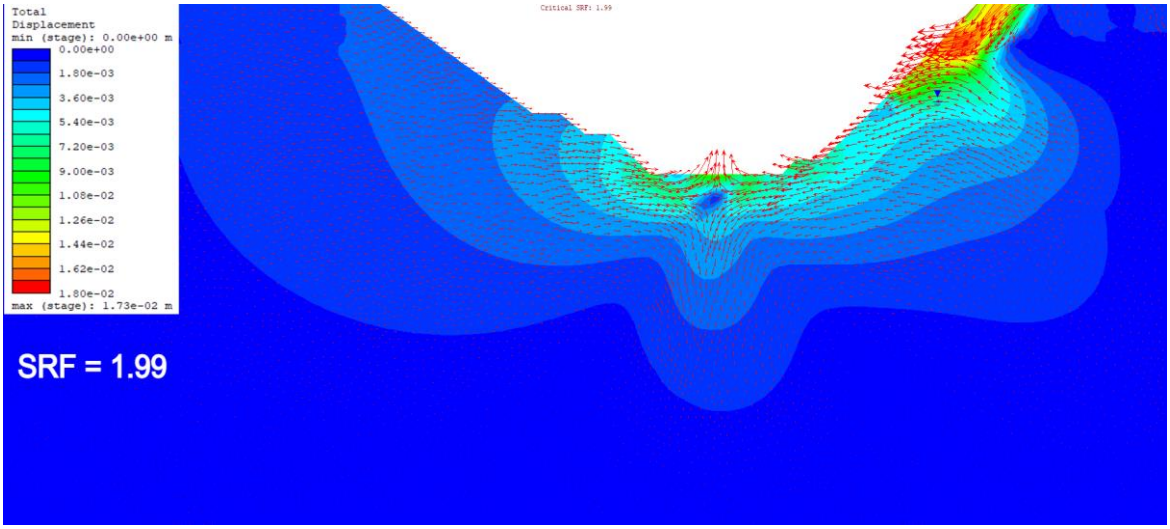

Figure 24. The calculated wall displacement field with increased elasticity modulus in production stage 2

4.3.2. Change in Cohesion

Reduced cohesion

As can be observed, the deformation and displacements that result are inversely proportional to the cohesion. Since cohesion was reduced to 1.5 MPa from 3.3 MPa, the displacements reached a higher maximum of 0.7 m given the critical SRF of 2.21. In comparison to the base case, the displacements doubled in magnitude. Another similar feature of the model is the progression of deformation on the south wall. The stress starts to accumulate around the top part of the wall, causing a major rock movement at the SRF of 2.4.

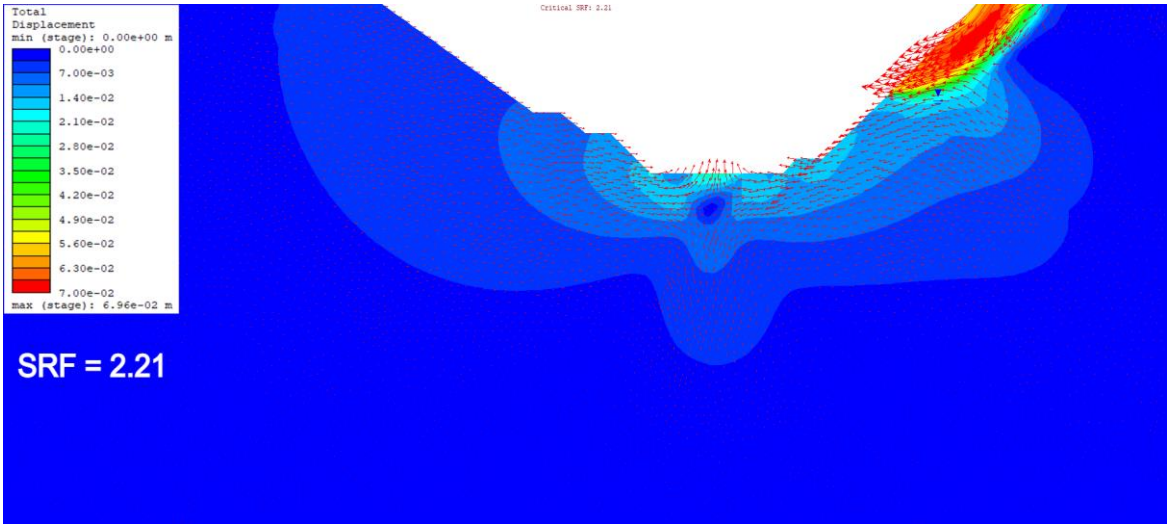

Figure 25. The calculated wall displacement field with reduced cohesion in production stage 2

Increased Cohesion

Due to the increase in cohesion from 3.32 MPa to 4.52 MPa, the displacements reached a greater maximum of 0.05 m when the critical SRF was 2.2. In comparison to the base scenario, the size of the displacements increased. Yet, it was assumed that the displacements would be comparatively lower than the base value due to their inverse proportionality. The evolution of

wall deformation on the south wall is nonetheless similar. With SRF = 2.7, the stress begins to collect near the top of the wall, causing significant rock displacement topping 5.4 m.

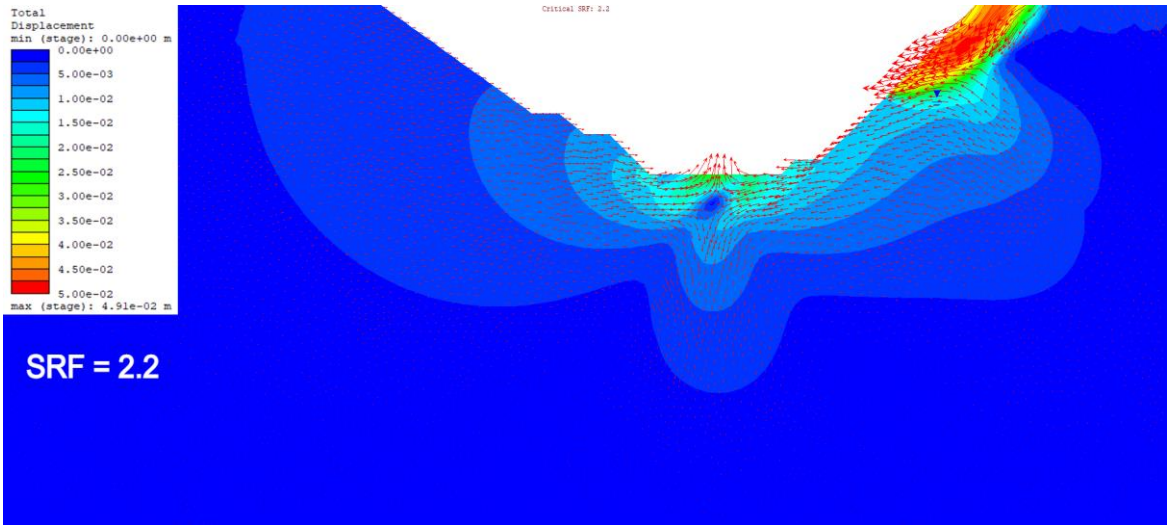

Figure 26. The calculated wall displacement field with increased cohesion in production stage 2

4.3.3. Change in Friction Angle

Reduced Friction Angle

It is worth noticing that a friction angle increase led to higher displacements compared to the base case results (see Fig. 27). Notwithstanding that the progression of deformation across the increasing SRF is the same, a change at the SRF of 1.6 is observable. At this stage, the wall is very stable and is not predicted to experience any major deformations. As SRF increases, reaching the critical value, the section of gabbro is predicted to displace up to 0.085 m.

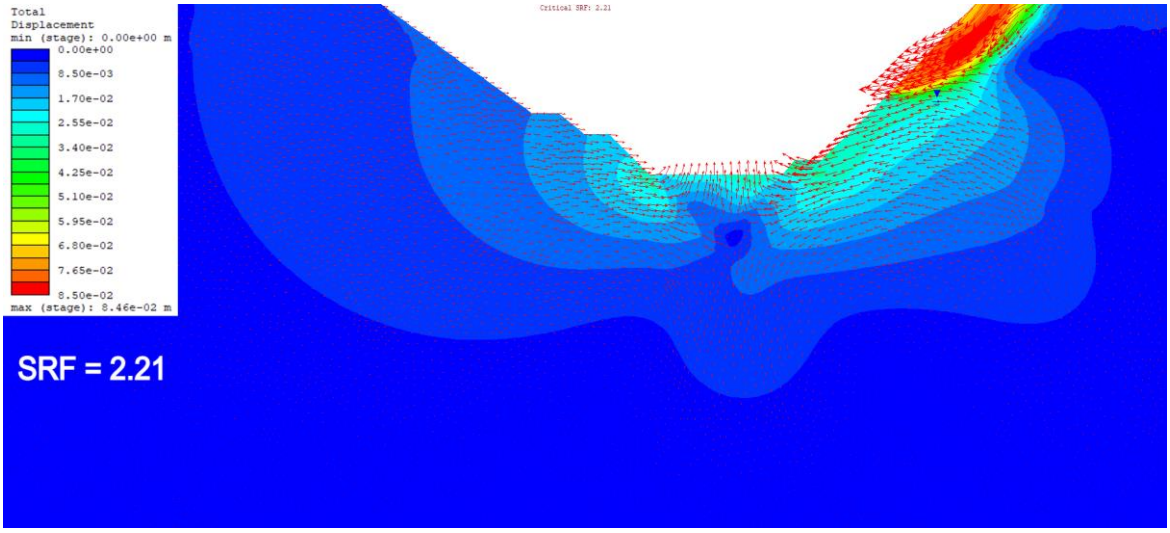

Figure 27. The calculated wall displacement field with reduced friction angle in production stage 2

Increased Friction Angle

The increase in friction angle of andesite, remarkably, resulted in higher displacements compared to base value, too. The maximum displacement of 0.065 m was established at critical SRF = 2.21. Apart from that, the Fig. 28 shows the similar slide mechanism as was illustrated in previous models of the production stage 2.

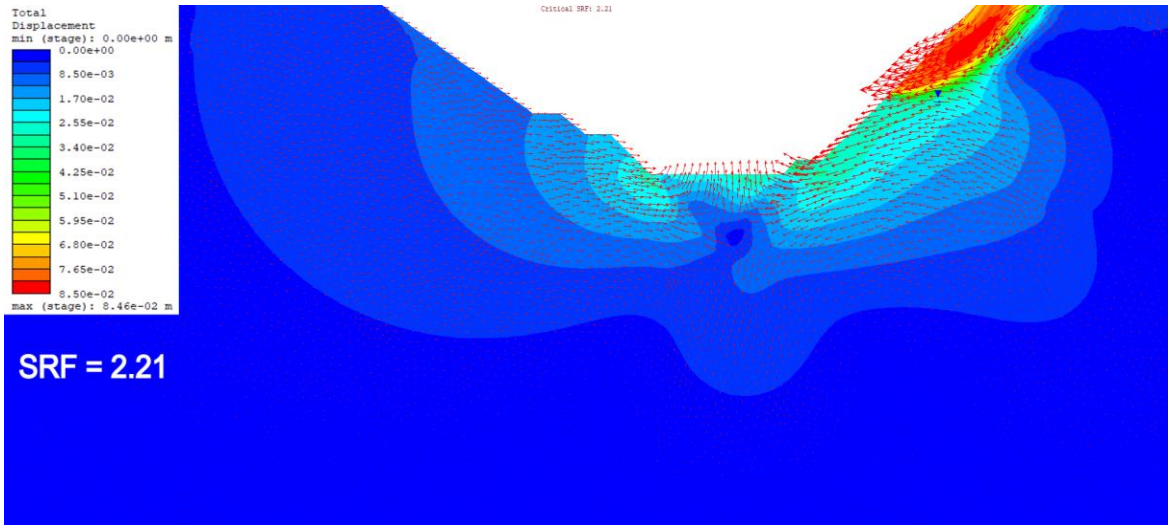

Figure 28. The calculated wall displacement field with increased friction angle in production stage 2

5. DISCUSSION

First of all, the analysis of base cases throughout the production stages clearly indicated the weaknesses on the south wall. This is the area, as mentioned, where the domains of gabbro and breccia intersect. The majority of the deformation zone, nonetheless, is caused by the movement of gabbro. It might be explained by the low intact rock parameters that the rock has. Hence, it resulted in weak rock mass properties. For example, the median UCS of gabbro is equal to 14 MPa, whereas andesite and breccia have 48 MPa and 43 MPa, respectively. All the production stages displayed similar failure mechanisms given the time dimension and stress-strength reduction technique. The mining activities induced higher magnitudes of stress levels in the bottom and lateral parts of the pit. Thus, higher displacements around these areas are observed. Ultimately, the stress-strength reduction method revealed possible moderate deformations on the south wall, reaching 0.14 m of rock movement. Thus, a trend of displacement and deformation growth in relation to the production progression becomes visible (see Table 7).

Table 7. Maximum total displacement fields observed at critical SRF in each production stage

Production stages	Critical SRF	Max. displacement at critical SRF (cm)
2	2.15	3.44
3	2.20	4.52
4-5	2.20	7.05
6	2.21	14.20

Nevertheless, Fig. 29 suggests that stages 4-5 might be more unstable than stage 6 beyond the critical SRF. Specifically, displacements up to 3.7 m are predicted, given the SRF = 2.4. Yet, this is the maximum value observed among all the stages. The graph also emphasizes the rapid growth in maximum displacements after the critical SRF in all cases. It was mentioned earlier

that the increase in SRF induces a growth in displacements and a major failure zone on the south wall, as we follow sections 3.2.2 and 2.4. Given the displacements at critical SRF (i.e., on the verge of failure), it is now possible to determine factors of safety that would ensure the best safety on the site. As can be observed, critical SRF for all production stages range between 2.15 and 2.21. Thus, FoS equal to or lower than these numbers might be the most convenient ones for the excavation. Nevertheless, the deformation boundaries of the stages indicate the possibility of minor rock fall, which is unarguably unpleasant for the production (see Appendices C, F, I, L). This can require additional minor support design and proper management.

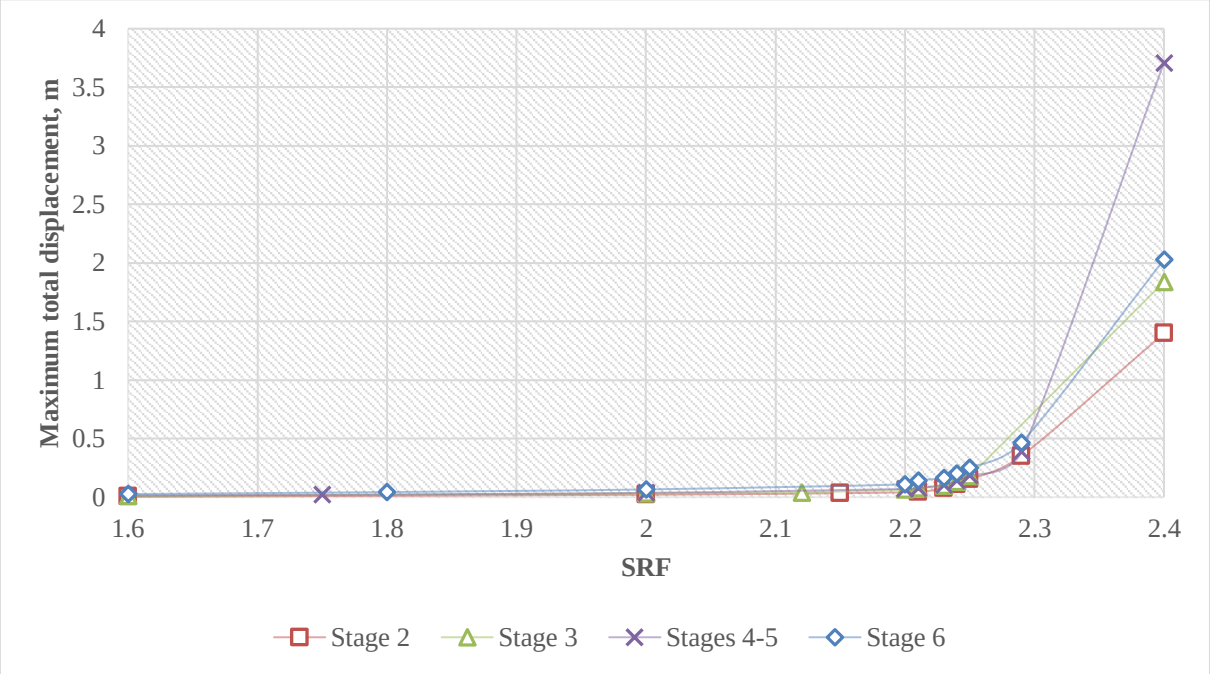

Figure 29. The chart of SRF against calculated maximum total displacement

Secondly, the sensitivity analysis demonstrates different impacts of the changes in rock mass properties. In particular, the alterations of Young's modulus displayed its inverse relationship with total displacement fields (see Table 8). The changes in cohesion, on the other hand, illustrated ambiguous effects on the model. Both increases and decreases in the cohesion of

andesite resulted in higher displacements compared to the base case. This trend also concerns friction angle, as the impact of the changes remains inconclusive. Eventually, this might indicate that the base magnitudes of cohesion and friction angle ensure the best stability (i.e., 3.3 MPa and 39.3 deg., respectively).

Table 8. Summarized results of the sensitivity analysis

Rock mass property	Change, %	Max. displacements at critical SRF (cm)	Critical SRF
Elasticity Modulus	-55	15.50	2.21
	0 (Base Value)	3.44	2.15
	+35	1.73	1.99
Cohesion	-55	6.96	2.21
	0 (Base Value)	3.44	2.15
	+35	4.91	2.20
Friction Angle	-55	8.60	2.21
	0 (Base Value)	3.44	2.15
	+35	6.91	2.21

6. CONCLUSIONS AND RECOMMENDATIONS

The conducted finite element analysis of the Bozshakol pit provided a range of critical information. That is, the required factors of safety, failure mechanisms, deformation zones and boundaries, displacement, and vectors based on the obtained results, the following conclusions are made:

- The south wall of the pit is more susceptible to higher displacements and deformations in comparison to the north wall of the pit. While the north wall had very minor movements ranging from 0 m up to 0.008 m, the south wall achieved the maximum of 0.035 m given the critical SRF, as in production stage 2. As SRF is enhanced to 2.6, the rock movement correspondingly increases to 3.3 m. Such a trend implies the necessity of maintaining FoS = 2.15 or lower.
- As the mining goes on, total displacement fields increase accordingly. This is observable from the mean and maximum displacements throughout the stages between 2 and 6 (see Table 7). The maximum movement is predicted to gradually increase from 0.035 m to 0.142 m starting from the current point up to the ultimate pit production. This implies the need to manage possible failures as early as possible. As time goes on, negligence or insufficient analysis of the stability of the slope may eventually result in major failures.
- Most of the displacements took place in the area where gabbro is situated. This, accordingly, indicates weaknesses in the rock. Low intact rock and rock mass parameters are the main reasons for such an outcome. In order to avoid this failure, a minor support design is needed in this area.
- Upwards movement from the pit bottom and downward slide of the rock from the lateral sides of the pit section is caused by the effects of mining activities (e.g., excavation, blasting, benching). It becomes clear from the results and graphics that this trend is present in all production stages.

Although the paper demonstrated fairly interesting and sufficient results, further work remains to be done. Specifically, the following recommendations are proposed:

- It is highly recommended that the project be developed using three-dimensional tools, too. As mentioned, three-dimensional models are capable of providing substantial information all across the pit and possible deformation zones. That would also make possible a comparative analysis with the results of the 2D FE analysis to distinguish the major differences and features.
- By using the results of this project and other geotechnical analyses (i.e., LEM, analytical, and empirical), it is advised to develop a convenient support design to avoid, minimize, or mitigate the impacts of the deformations displayed in this thesis.
- It is also recommended to analyze other sections of the pit that could be prone to deformation zones. Multiple numerical calculations would assist in having a broader look at the critical areas of the pit.
- It could be interesting to conduct a sensitivity analysis by changing other properties apart from rock mass parameters. There are, undoubtedly, other factors that highly influence the stability of the slope. For example, alterations in the overall slope angle, groundwater level, Poisson's ratio, and tensile strength could demonstrate their impacts on the model.

7. REFERENCES

Bar, N., & Barton, N. (2017). The Q-Slope Method for Rock Slope Engineering. *Rock Mechanics and Rock Engineering*, *50*(12), 3307–3322. https://doi.org/10.1007/s00603-017-1305-0

Barton, N. (2013). Shear strength criteria for rock, rock joints, rockfill and rock masses: Problems and some solutions. *Journal of Rock Mechanics and Geotechnical Engineering*, *5*(4), 249–261. https://doi.org/10.1016/j.jrmge.2013.05.008

Bieniawski, Z. (1993). Classification of Rock Masses for Engineering: The RMR System and Future Trends. *Elsevier EBooks*, 553–573. https://doi.org/10.1016/b978-0-08-042066-0.50028-8

Blake, W. (1966). Application of the finite element method of analysis in solving boundary value problems in rock mechanics. *International Journal of Rock Mechanics and Mining Sciences & Geomechanics Abstracts*. https://doi.org/10.1016/0148-9062(66)90021-0

Chiwaye, H. T., & Stacey, T. (2010). A comparison of limit equilibrium and numerical modelling approaches to risk analysis for open pit mining. *Journal of the South African Institute of Mining and Metallurgy*, *110*(10), 571–580. http://www.scielo.org.za/pdf/jsaimm/v110n10/02.pdf

Cook, R. D., Malkus, D. S., Plesha, M. E., & Witt, R. J. (2001). *Concepts and Applications of Finite Element Analysis*. John Wiley & Sons Incorporated.

Duncan, J. S. (1996). State of the Art: Limit Equilibrium and Finite-Element Analysis of Slopes. *Journal of Geotechnical Engineering*, *122*(7), 577–596. https://doi.org/10.1061/(asce)0733-9410(1996)122:7(577

Hammah, R., Curran, J., Yacoub, T., & Corkum, B. T. (2004). Stability Analysis of Rock Slopes using the Finite Element Method. *RocScience*.

Frankovská, J., Kopecký, M., Panuška, J., & Chalmovský, J. (2015). Numerical Modelling of Slope Instability. *Procedia Earth and Planetary Science*. https://doi.org/10.1016/j.proeps.2015.08.076

Griffiths, D. V., & Lane, P. A. (2001). Slope stability analysis by finite elements. *Geotechnique*, *51*(7), 653–654. https://doi.org/10.1680/geot.51.7.653.51390

Hoek, E., & Marinos, P. (2007). A brief history of the development of the Hoek-Brown failure criterion. *Soils & Rocks*, *30*(2), 85–95. https://doi.org/10.28927/sr.302085

Jing, L., & Hudson, J. B. (2002). Numerical methods in rock mechanics. *International Journal of Rock Mechanics and Mining Sciences*, *39*(4), 409–427. https://doi.org/10.1016/s1365-1609(02)00065-5

Kaczmarek, Ł., & Popielski, P. (2019). Selected components of geological structures and numerical modelling of slope stability. *Open Geosciences*, *11*(1), 208–218. https://doi.org/10.1515/geo-2019-0017

Khaburi, M., & Mortazavi, A. (2019). Slope Stability Analysis of Sarcheshmeh Copper Mine West Wall Under Seismic Loads. *Geotechnical and Geological Engineering*. https://doi.org/10.1007/s10706-019-00830-3

Labuz, J. F., & Zang, A. (2012). Mohr–Coulomb Failure Criterion. *Rock Mechanics and Rock Engineering*, *45*(6), 975–979. https://doi.org/10.1007/s00603-012-0281-7

Liu, S., Shao, L., & Li, H. (2015). Slope stability analysis using the limit equilibrium method and two finite element methods. *Computers and Geotechnics*, *63*, 291–298. https://doi.org/10.1016/j.compgeo.2014.10.008

Martin, D., & Stacey, P. (2017). *Guidelines for Open Pit Slope Design in Weak Rocks*. CRC Press.

Matthews, C. M., Farook, Z., & Helm, P. J. (2014). Slope stability analysis - limit equilibrium or the finite element method? .

Obregon, C., & Mitri, H. S. (2019). Probabilistic approach for open pit bench slope stability analysis – A mine case study. *International Journal of Mining Science and Technology*, *29*(4), 629–640. https://doi.org/10.1016/j.ijmst.2019.06.017

Puzrin, A. M., Alonso, E., & Pinyol, N. M. (2010). Geomechanics of Failures. *Springer EBooks*. https://doi.org/10.1007/978-90-481-3531-8

Rao, S. S. (2017). *The Finite Element Method in Engineering*. Butterworth-Heinemann.

Read, J., & Stacey, P. (2009). *Guidelines for Open Pit Slope Design*. CSIRO PUBLISHING.

Wiles, T. (2006). Reliability of numerical modelling predictions. *International Journal of Rock Mechanics and Mining Sciences*. https://doi.org/10.1016/j.ijrmms.2005.08.001

Zienkiewicz, O. C., Humpheson, C., & Lewis, R. W. (1976). Associated and non-associated viscoplasticity and plasticity in soil mechanics. 14F, 3T, 42R. *International Journal of Rock Mechanics and Mining Sciences & Geomechanics Abstracts*, *13*(3), 24. https://doi.org/10.1016/0148-9062(76)90443-5

Zienkiewicz, O. C., Taylor, R. J. K., & Fox, D. A. (2014). The Finite Element Method for Solid and Structural Mechanics. *Elsevier EBooks*. https://doi.org/10.1016/c2009-0-26332-x

8. APPENDICES

Appendix A. Maximum principal stress (Sigma 1) distribution in production stage 2

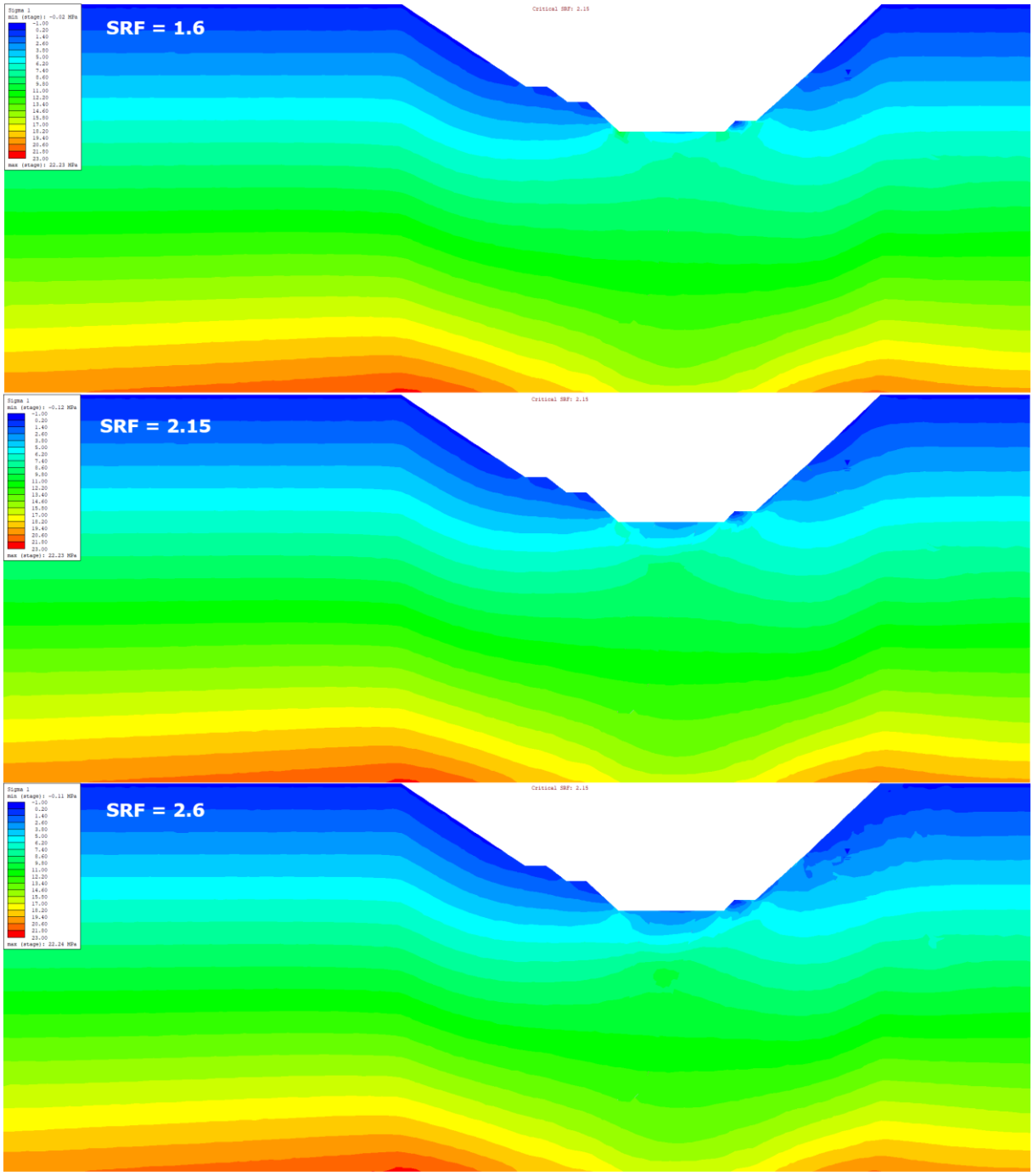

Appendix B. Maximum principal stress (Sigma 3) distribution in production stage 2

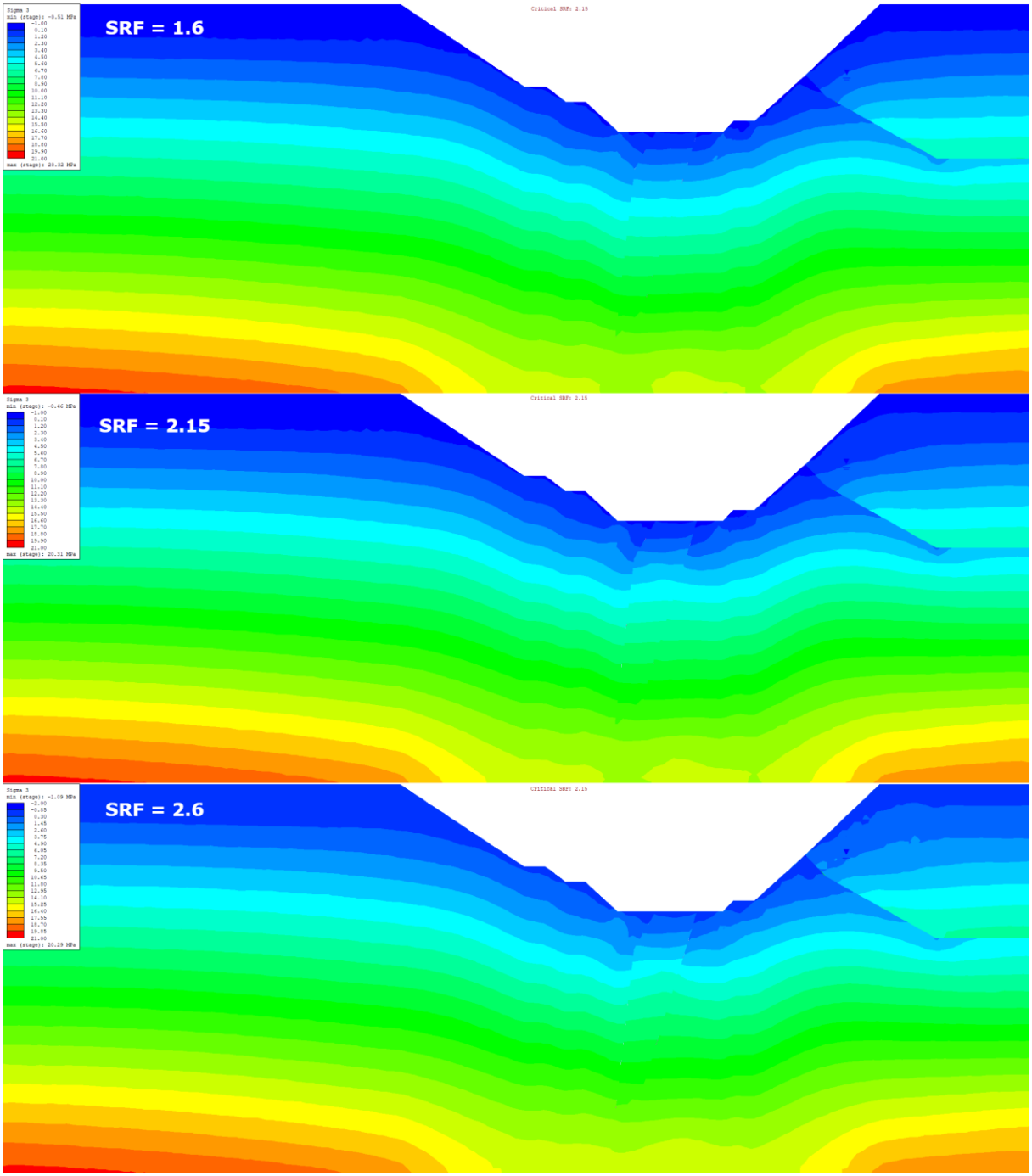

Appendix C. Deformed mesh boundaries in stage 2

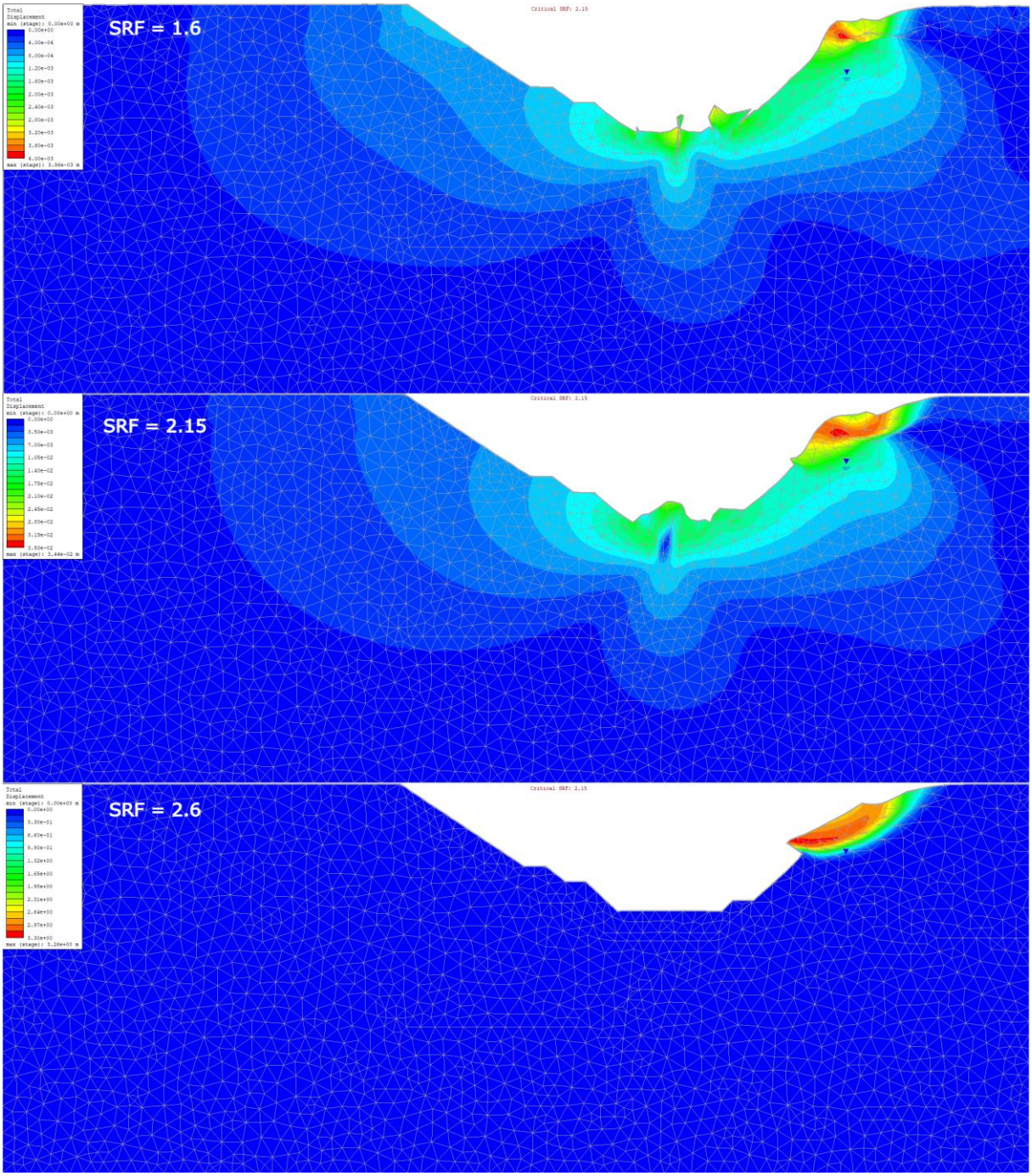

Appendix D. Maximum principal stress (Sigma 1) distribution in production stage 3

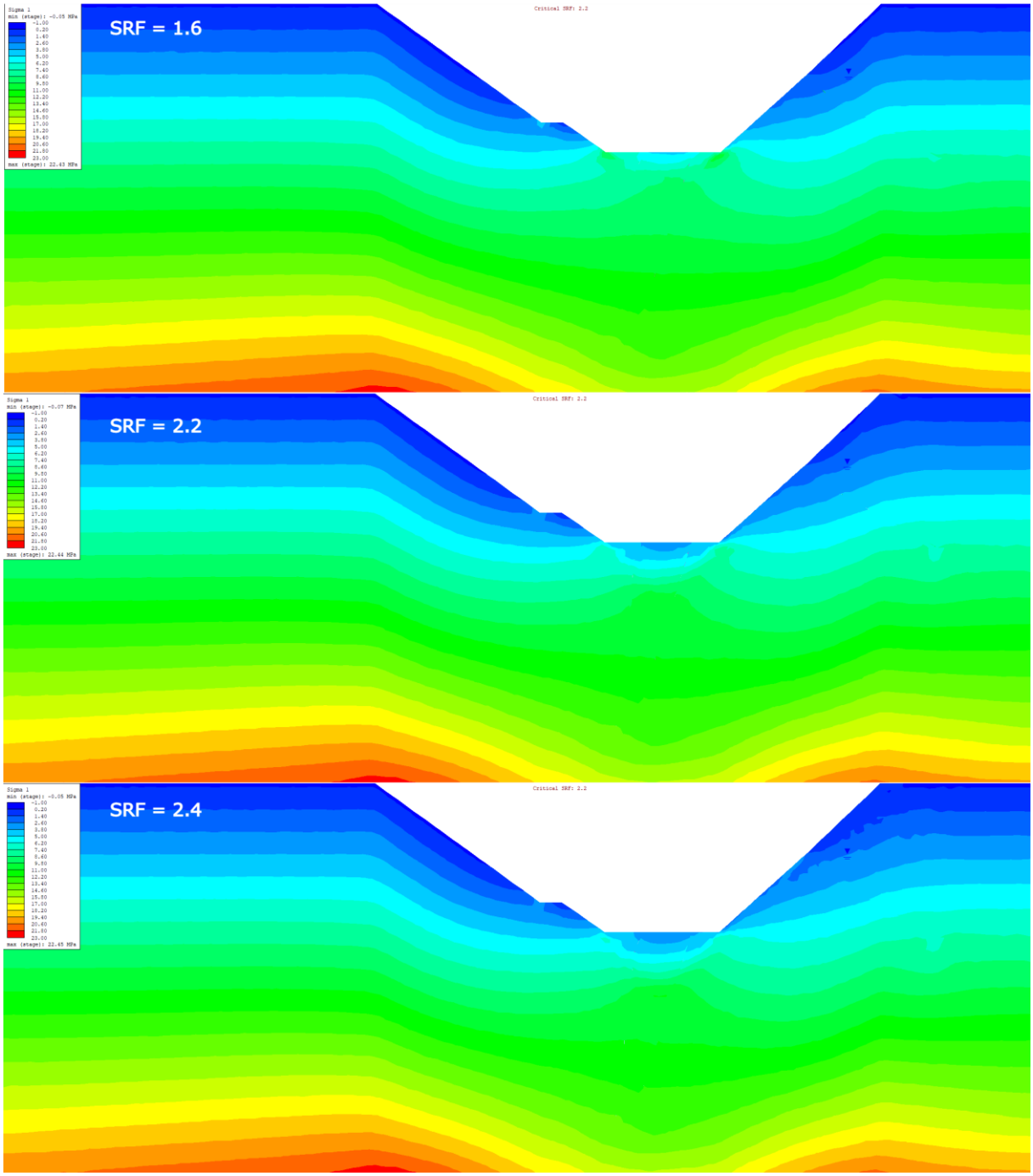

Appendix E. Maximum principal stress (Sigma 3) distribution in production stage 3

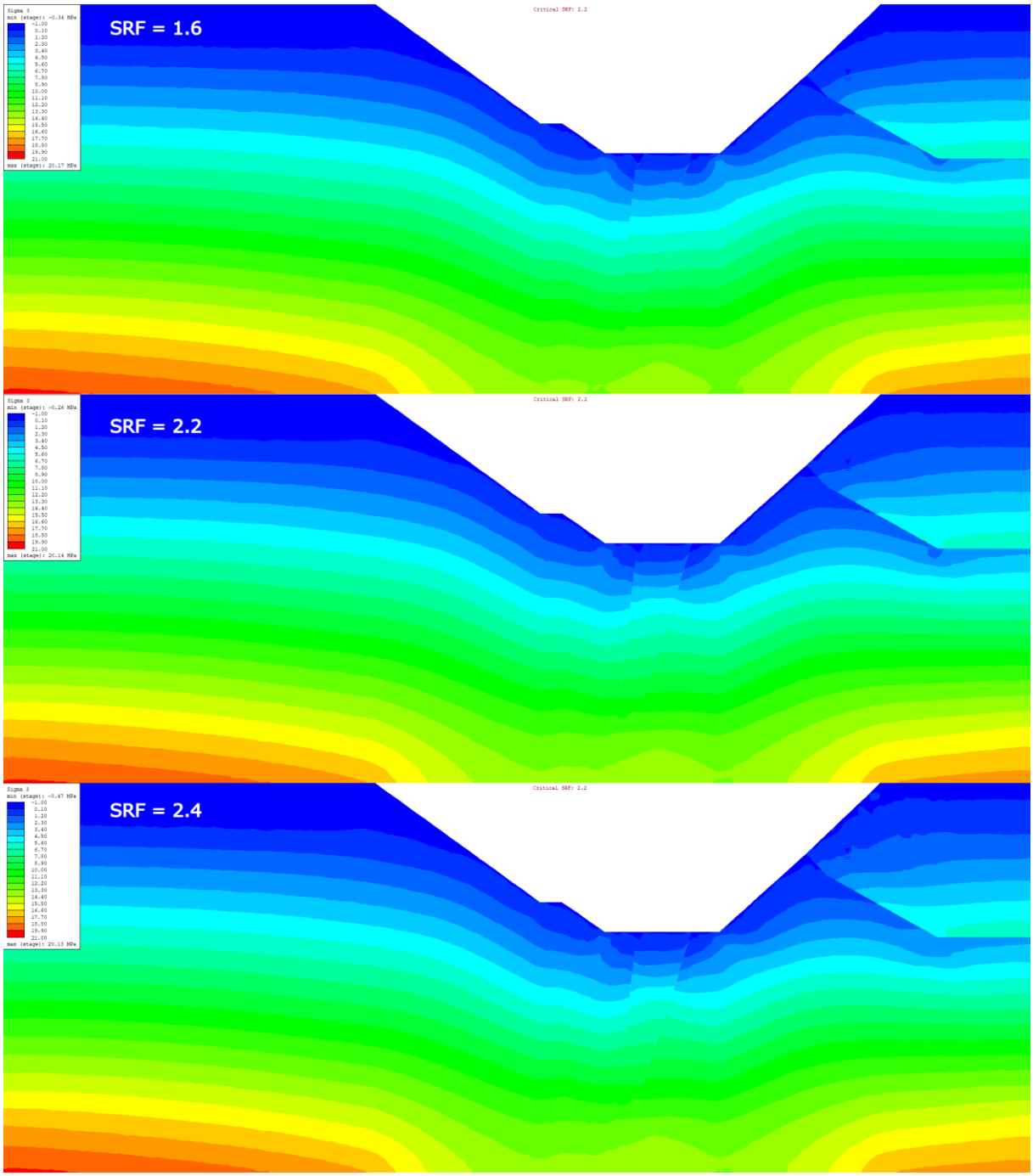

Appendix F. Deformed mesh boundaries in stage 3

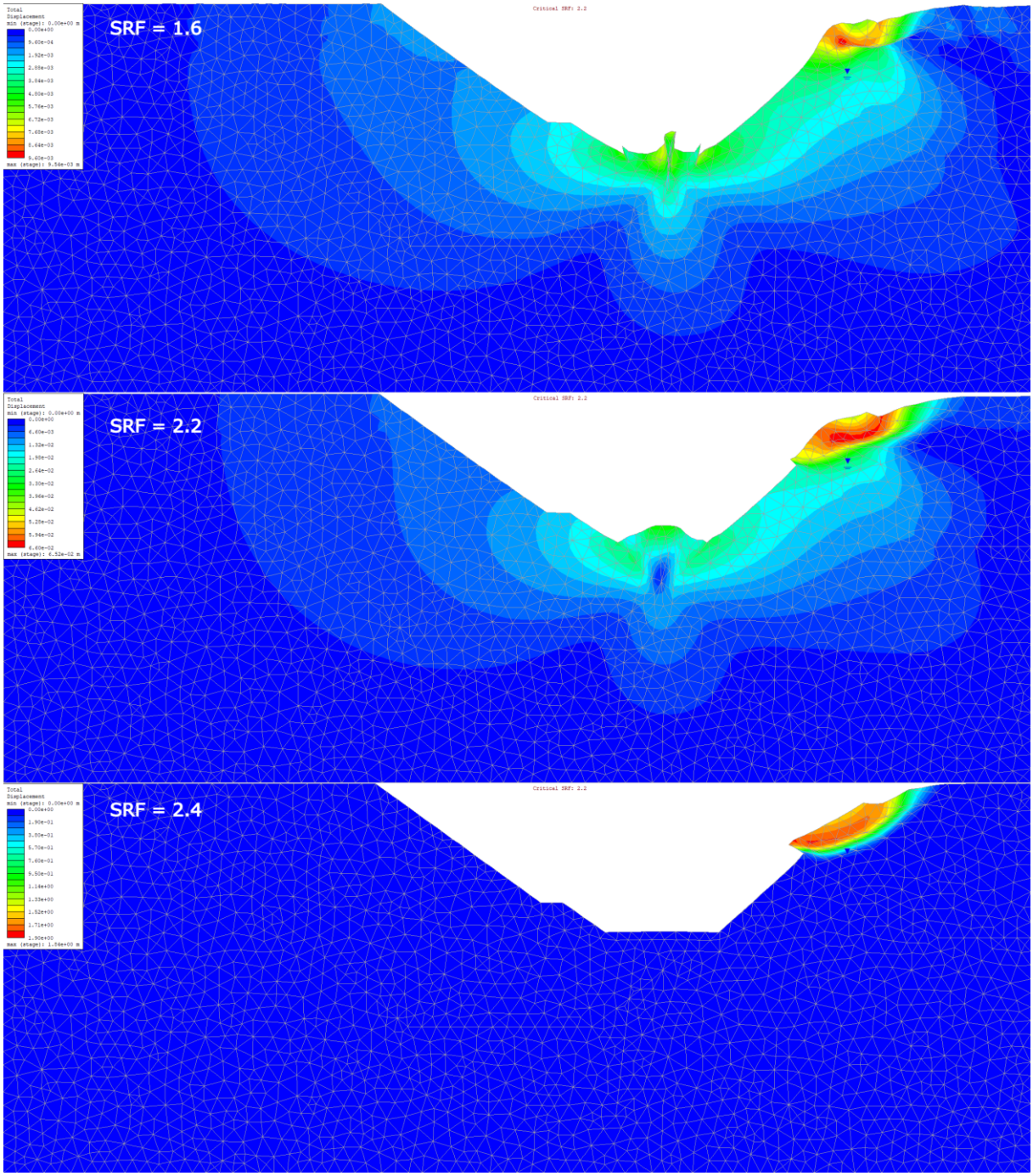

Appendix G. Maximum principal stress (Sigma 1) distribution in production stages 4-5

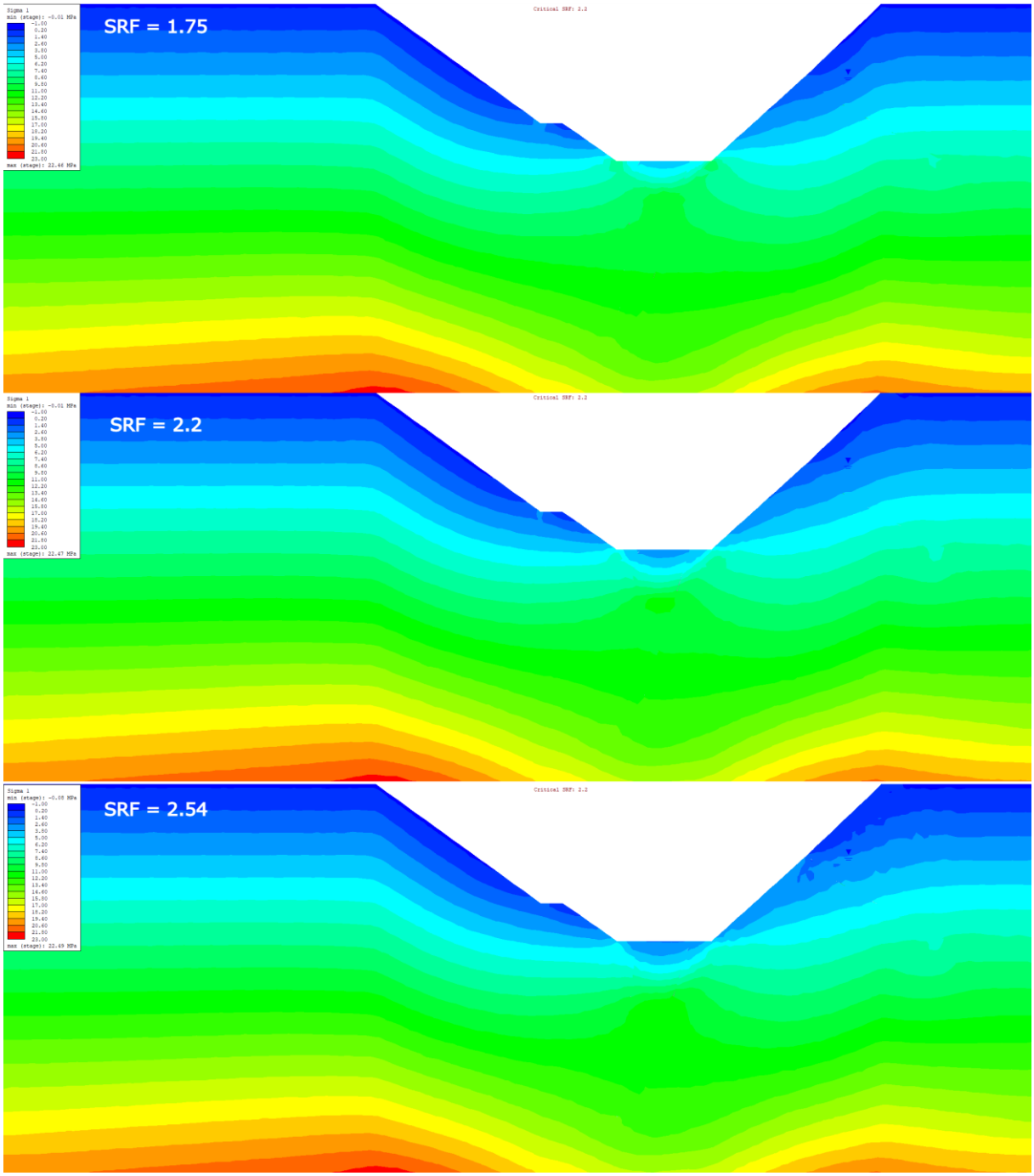

Appendix H. Maximum principal stress (Sigma 3) distribution in production stages 4-5

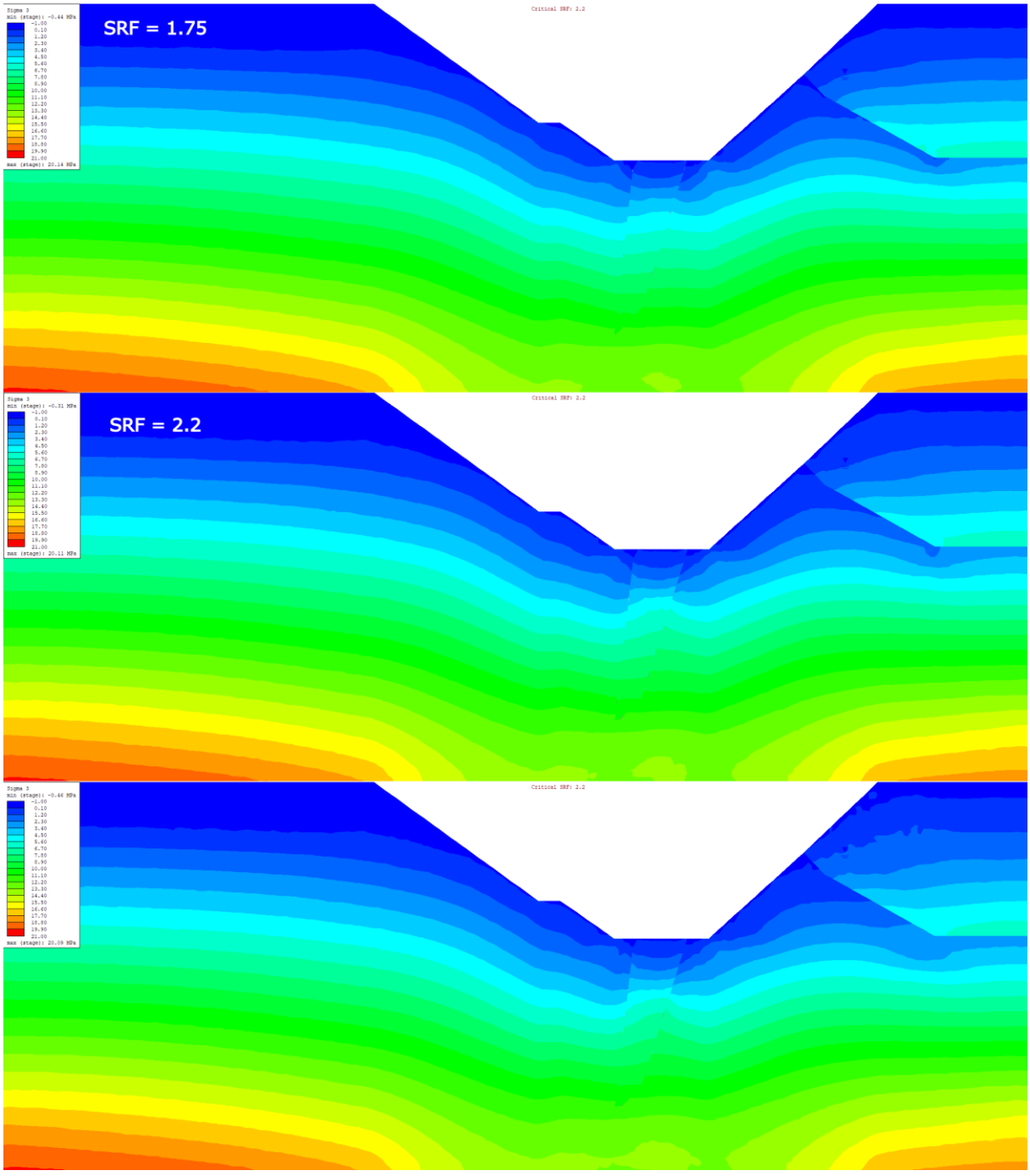

Appendix I. Deformed mesh boundaries in stages 4-5

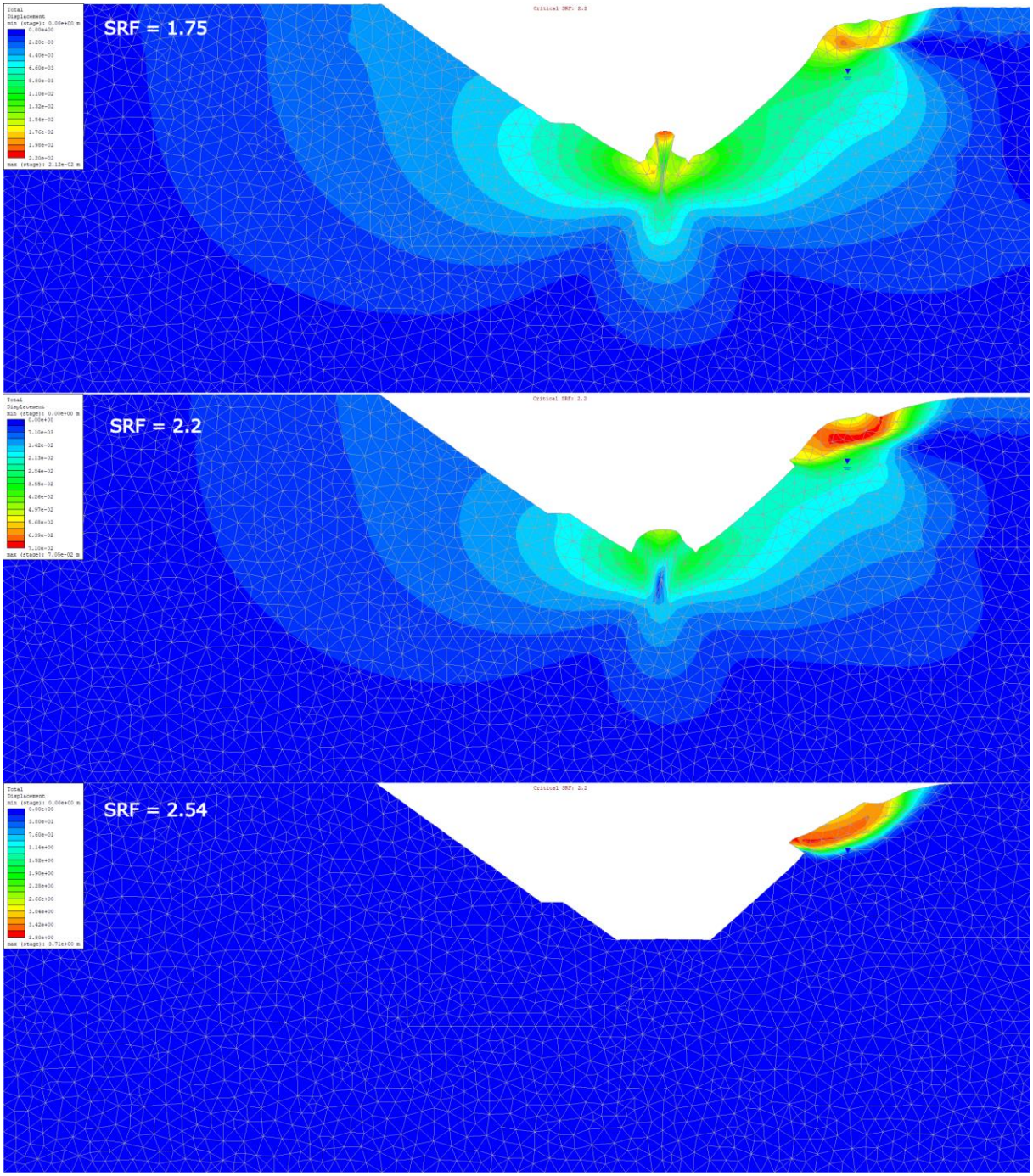

Appendix J. Maximum principal stress (Sigma 1) distribution in production stage 6

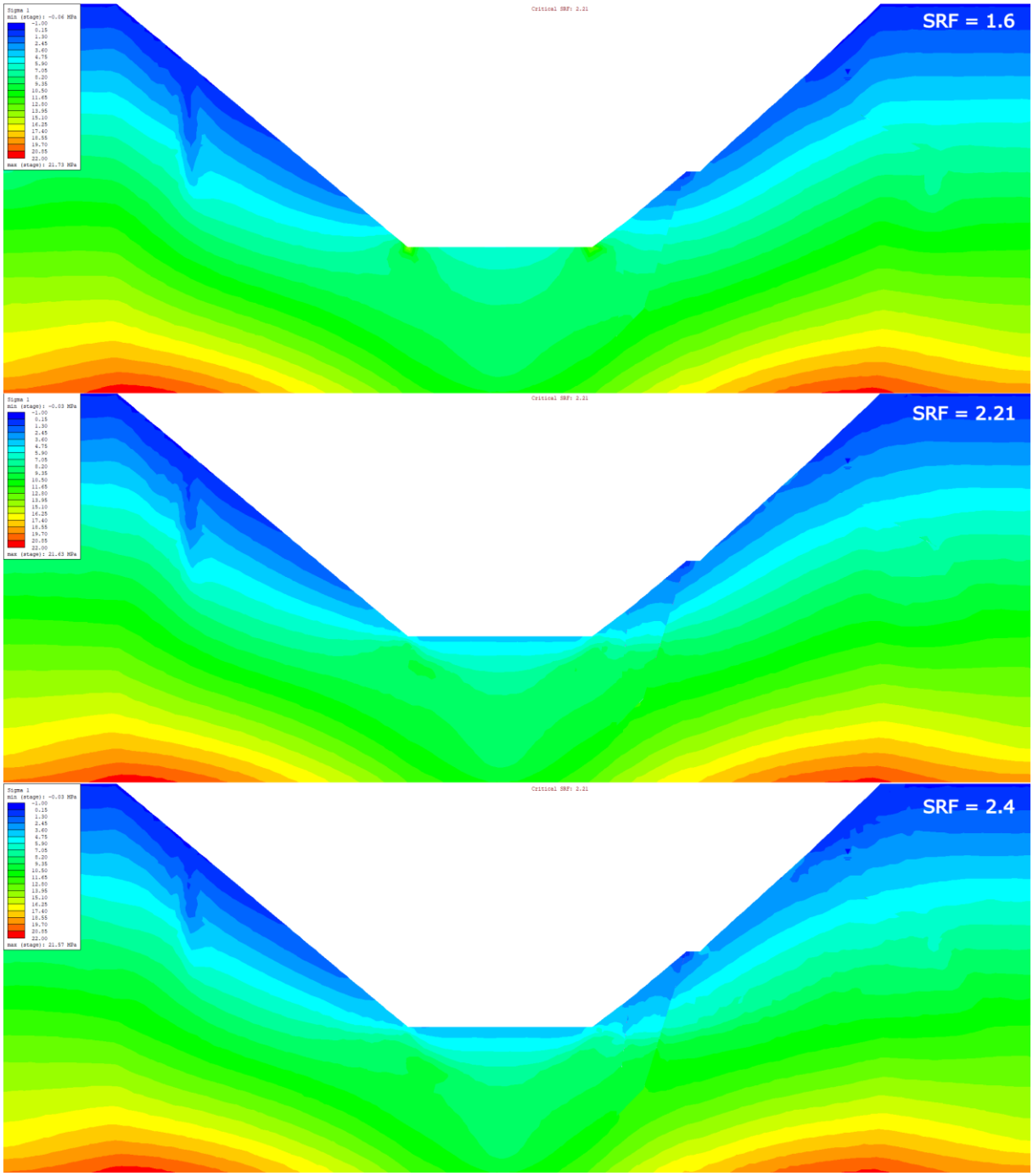

Appendix K. Maximum principal stress (Sigma 3) distribution in production stage 6

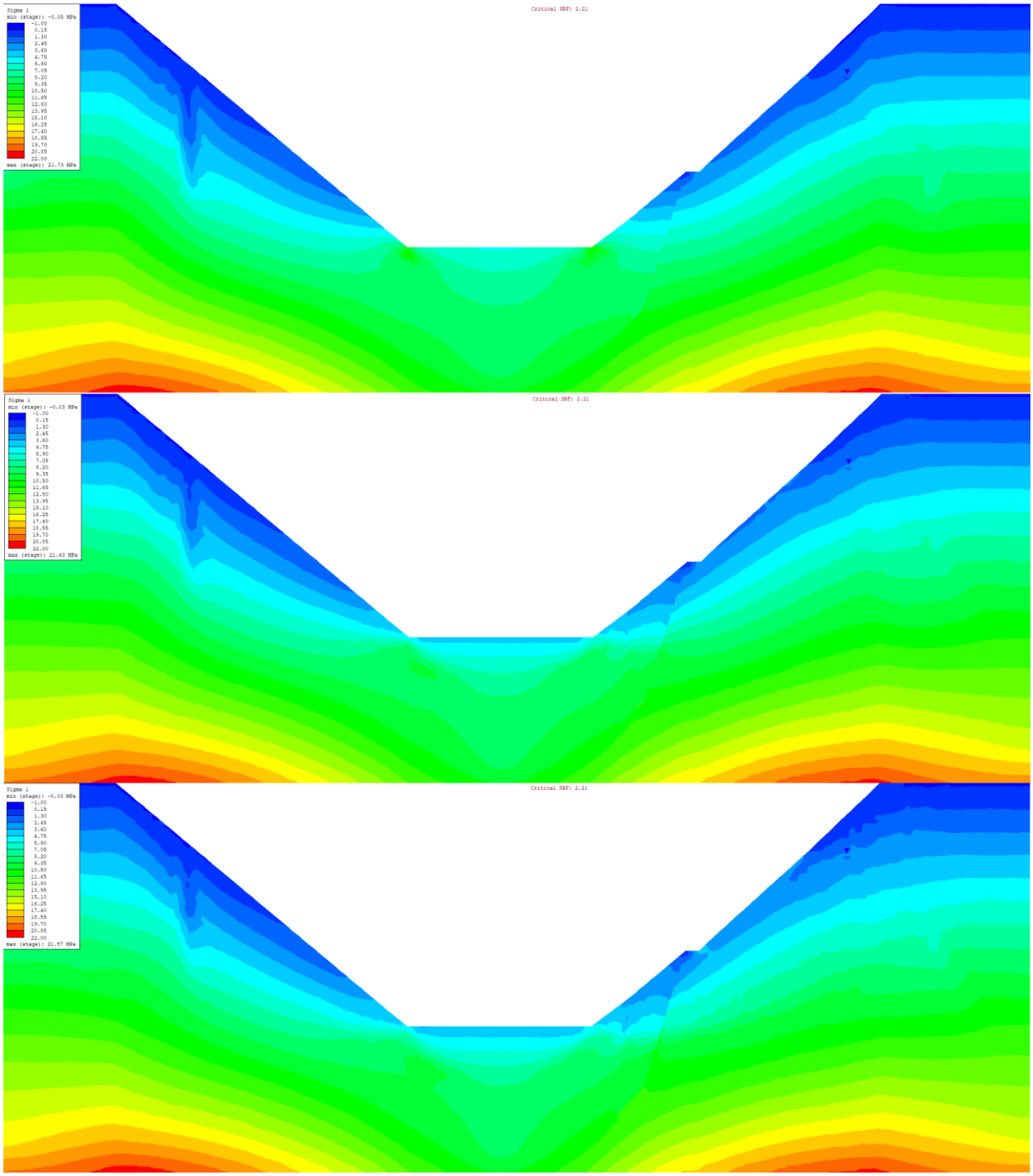

Appendix L. Deformed mesh boundaries in stage 6